IR Camera Techniques for Measuring Atmospheric Gases and Particles

Dr Fred Prata

Atmosphere and Climate Department

NILU

Reference material

Manual of Remote Sensing - 3 Volumes

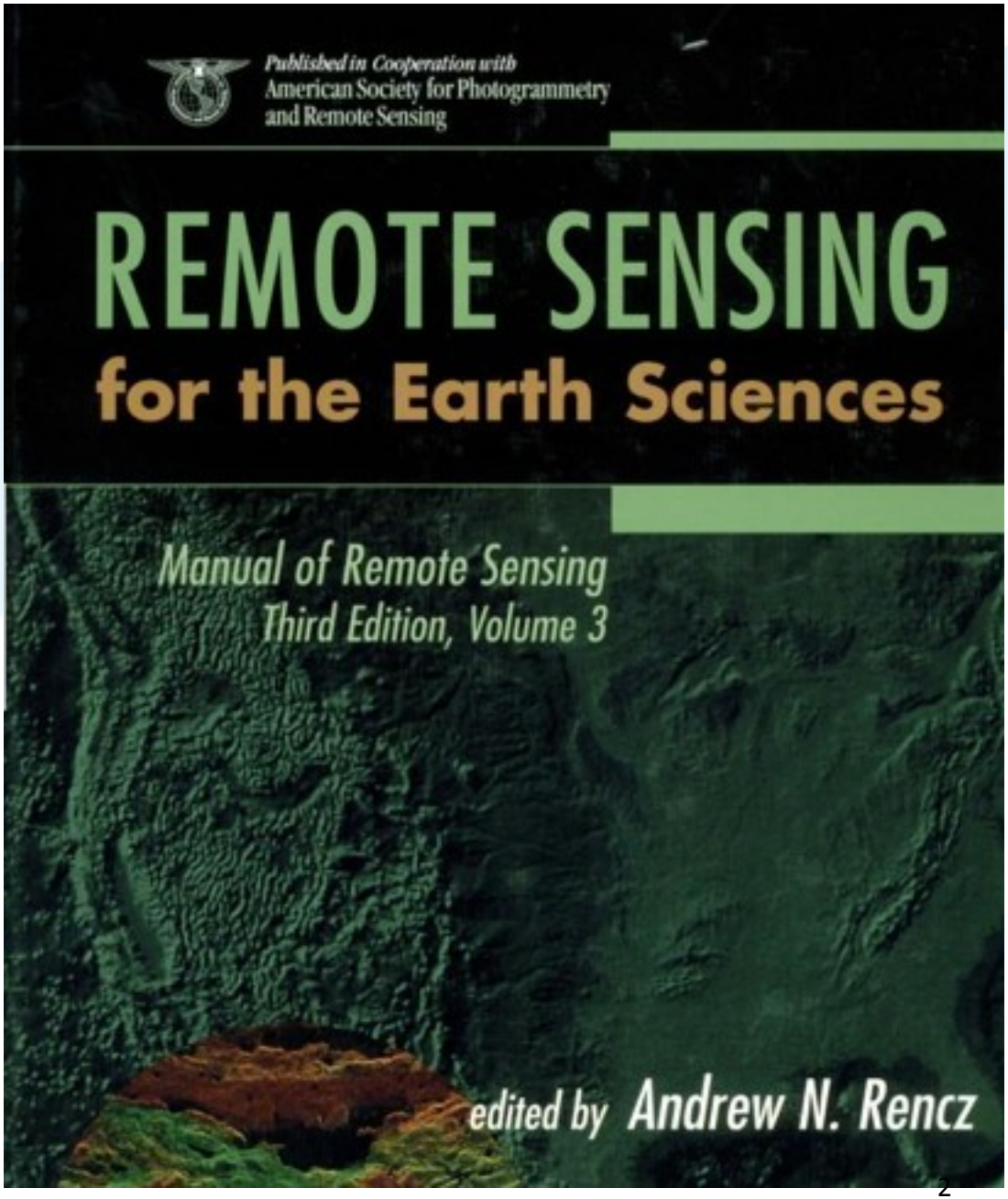

NILU

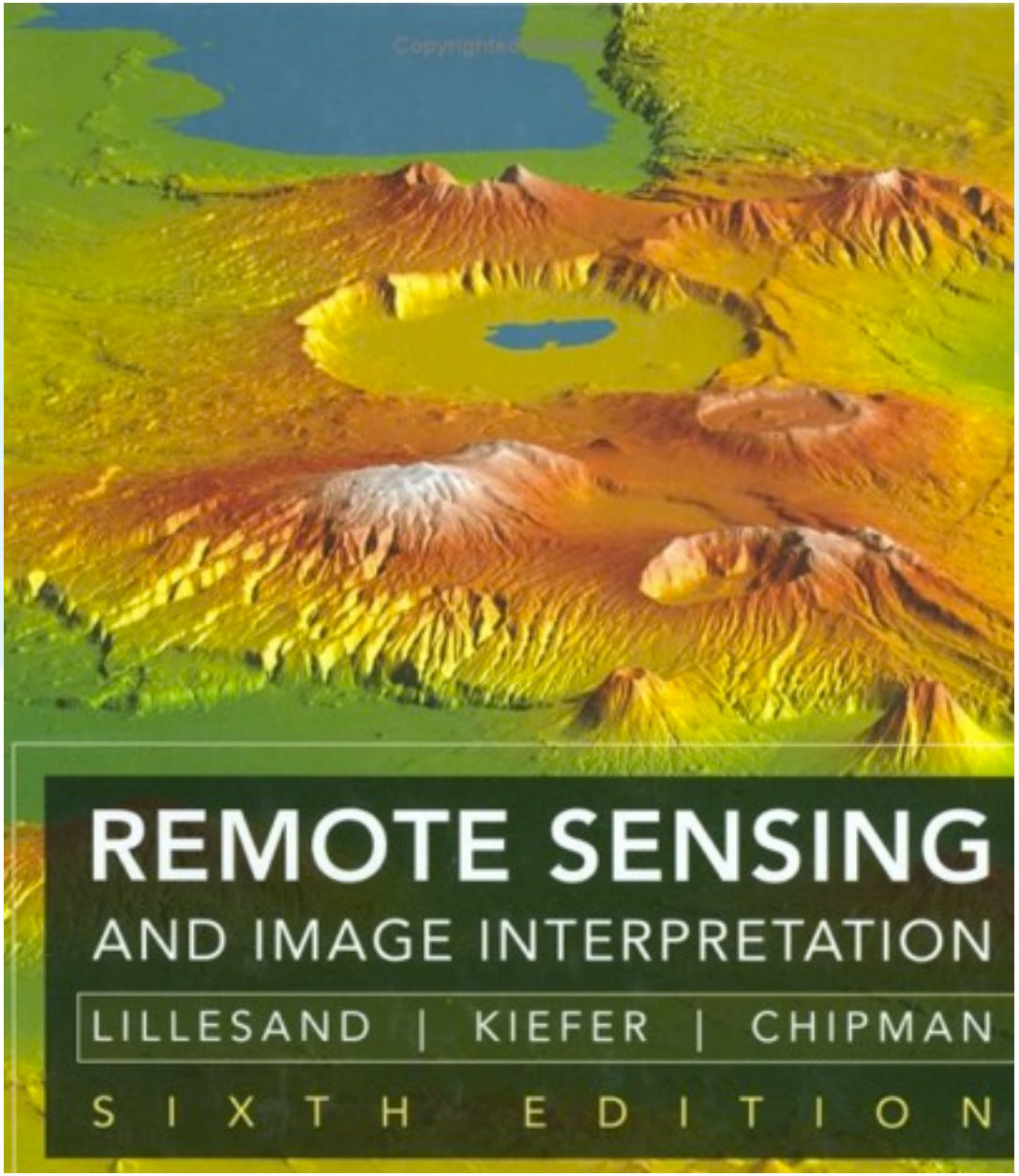
REMOTE SENSING
AND IMAGE INTERPRETATION
LILLESAND | KIEFER | CHIPMAN
SIXTH EDITION

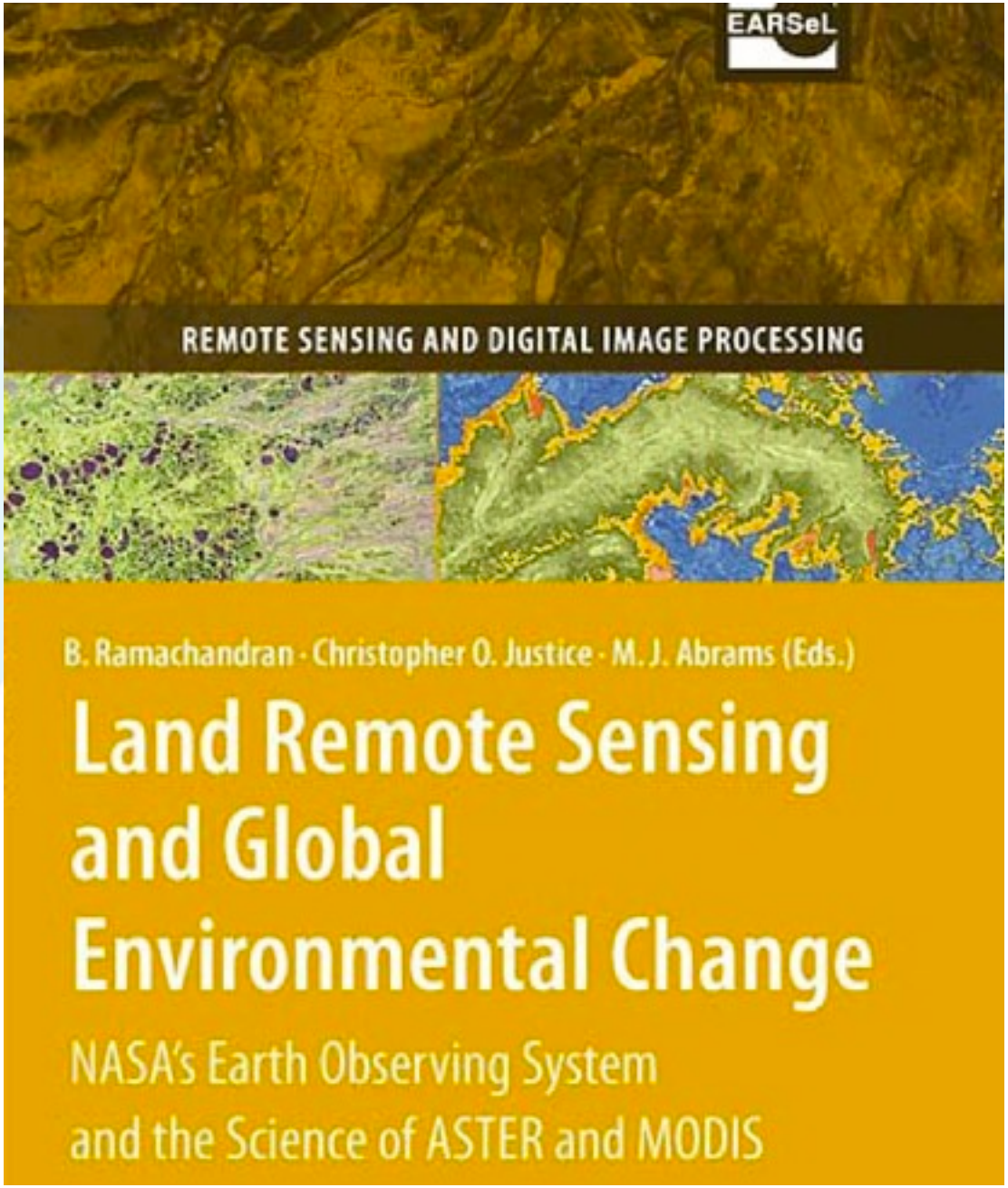
EARSeL
REMOTE SENSING AND DIGITAL IMAGE PROCESSING
B. Ramachandran · Christopher O. Justice · M. J. Abrams (Eds.)
Land Remote Sensing and Global Environmental Change
NASA's Earth Observing System and the Science of ASTER and MODIS

NILU

Optical and Atmospheric Remote Sensing

Remote Sensing: Optics and Optical Systems - Philip Slater, Addison-Wesley Educational Publishers Inc (December 1980), 592 pp. **ISBN-10:** 0201072505

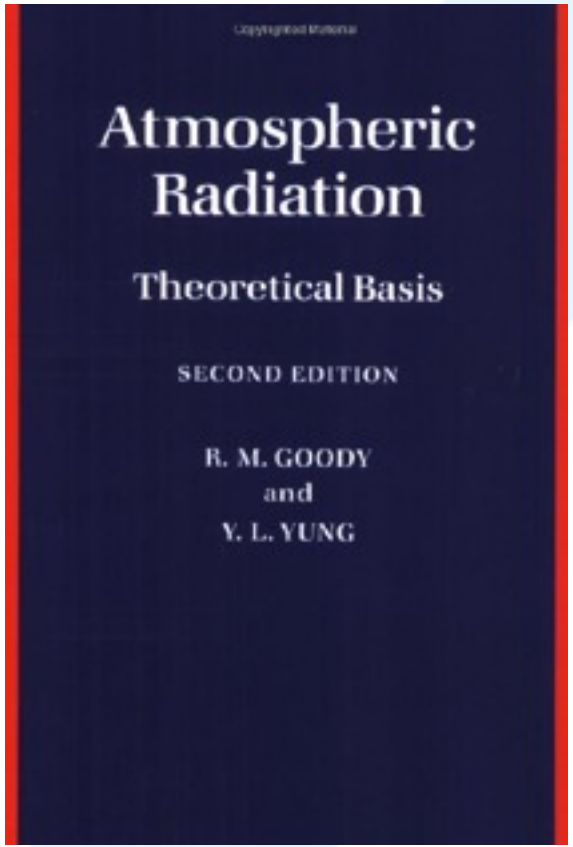

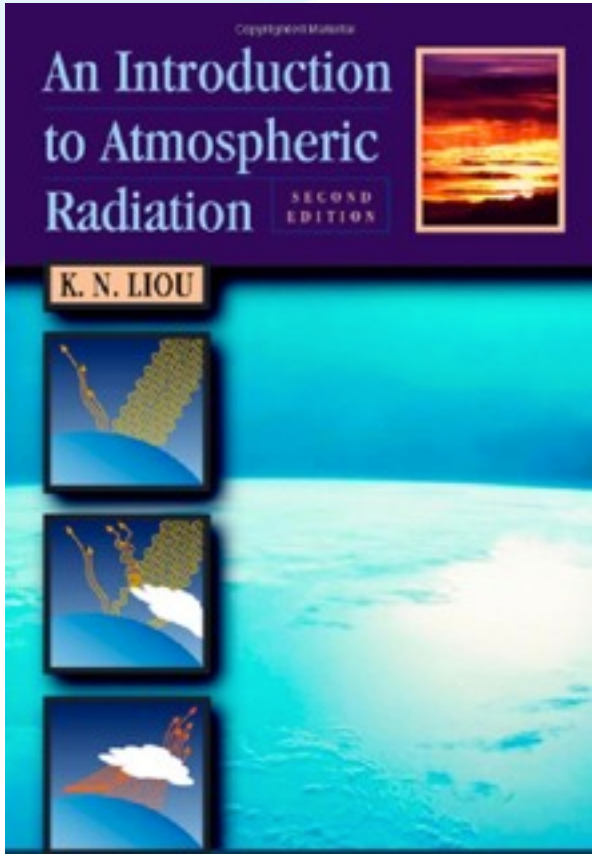

Some applications of thermal IR imaging

- Night vision - military and civilian applications
- Pipeline gas and leak detection
- Heat loss & insulation
- Road weather hazard detection systems
- Sport (?)

NILU

Surveillance

RAZIR
Mini IR Camera

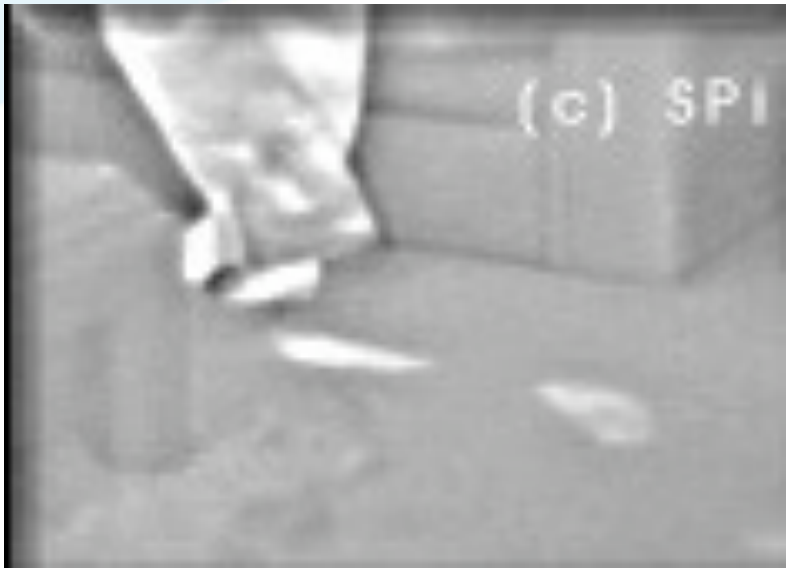

NILU

Heat loss/insulation

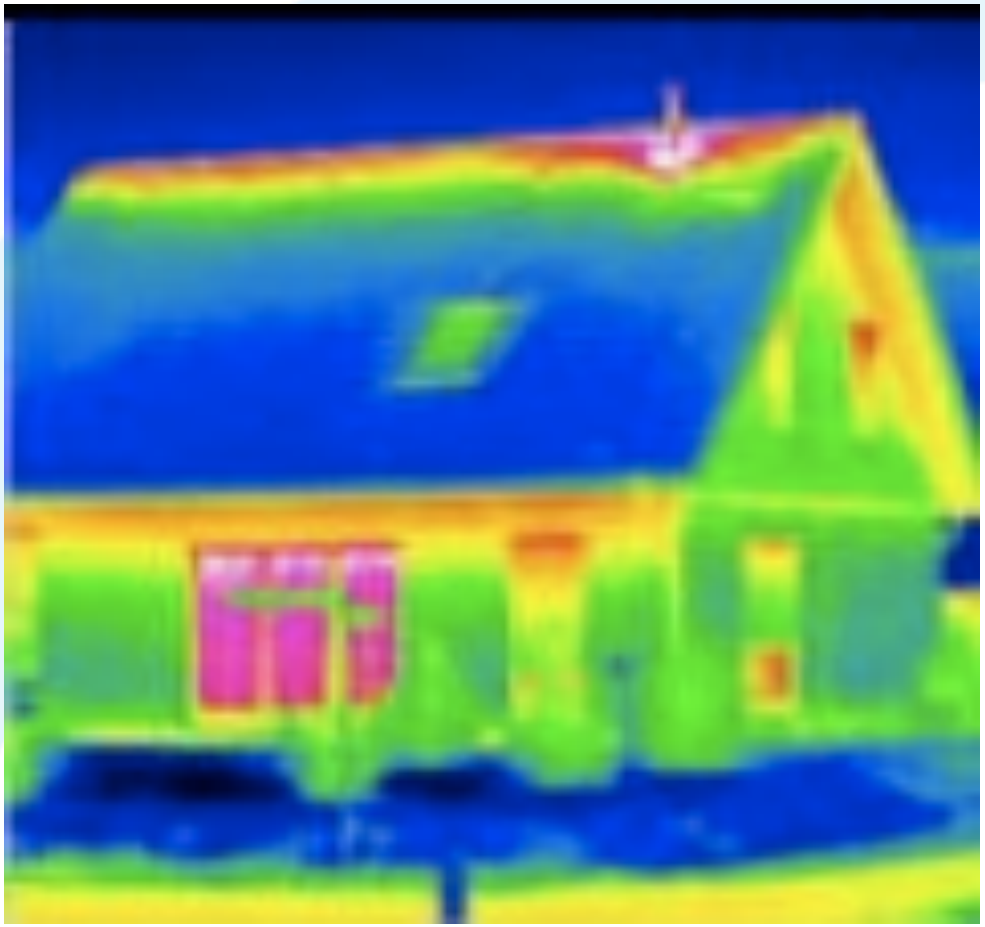

NILU

Leak detection - VOCs

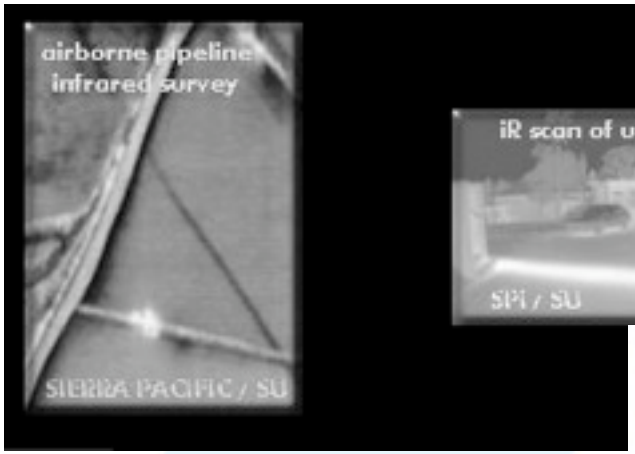

Figure 1B. The FLIR GasFindIR camera.

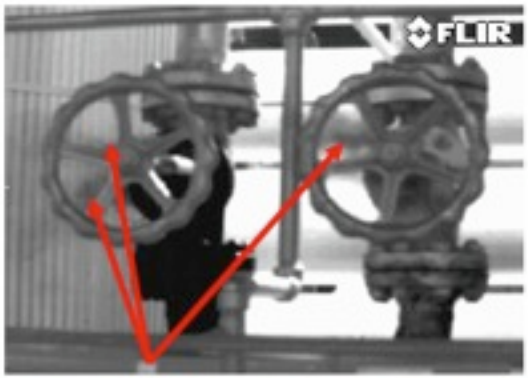

Figure 2A. Gas leaking from two valves. Arrows indicate gas plumes.

Figure 2B. Gasoline vapors wafting from the nozzle of a non-vapor recovery hose.

Road sensor technologies

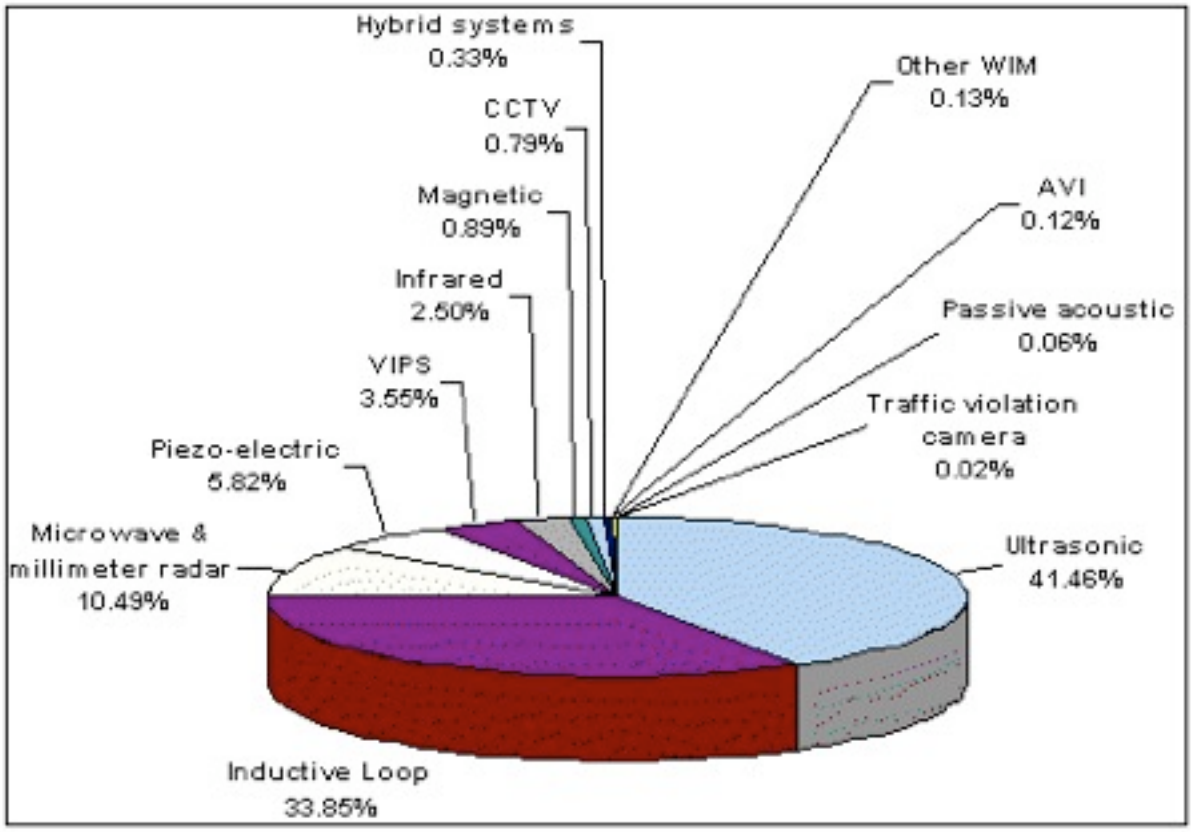

Chart 2.1.2 Global ATD Technology Market Share by Lanes Monitored

NILU

Road weather hazards

Video surveillance technologies such as this one showing vehicles passing a black ice warning flasher can provide improved warnings and advice to drivers and, when monitored in traffic centers, offer more rapid emergency response and incident management.

NILU

Response to Chemicals

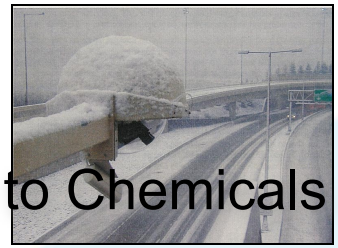

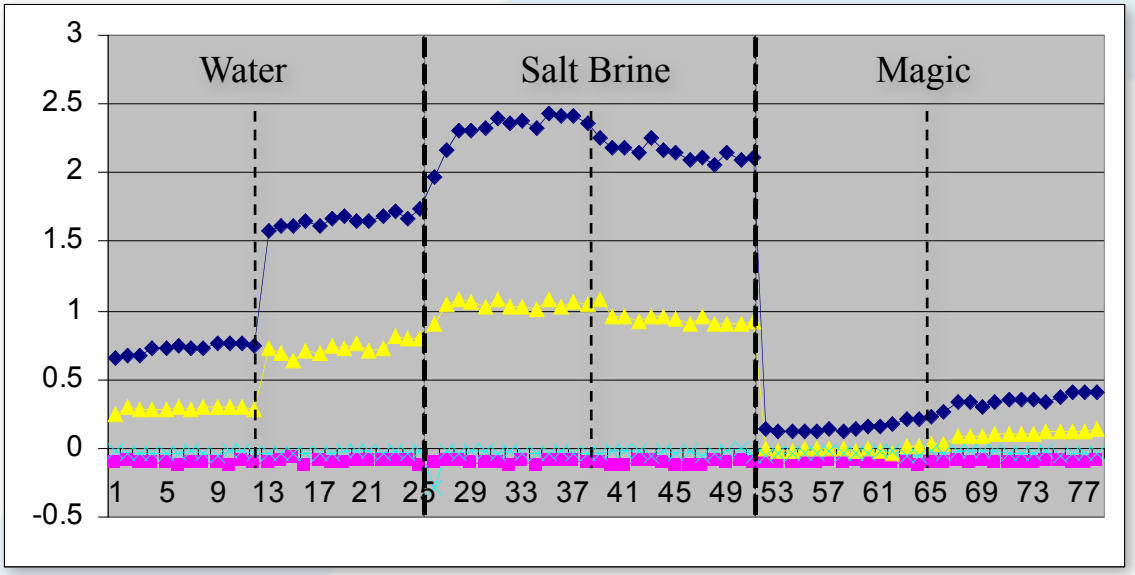

NILU

Night vision

NILU

The (wonderful) game of cricket

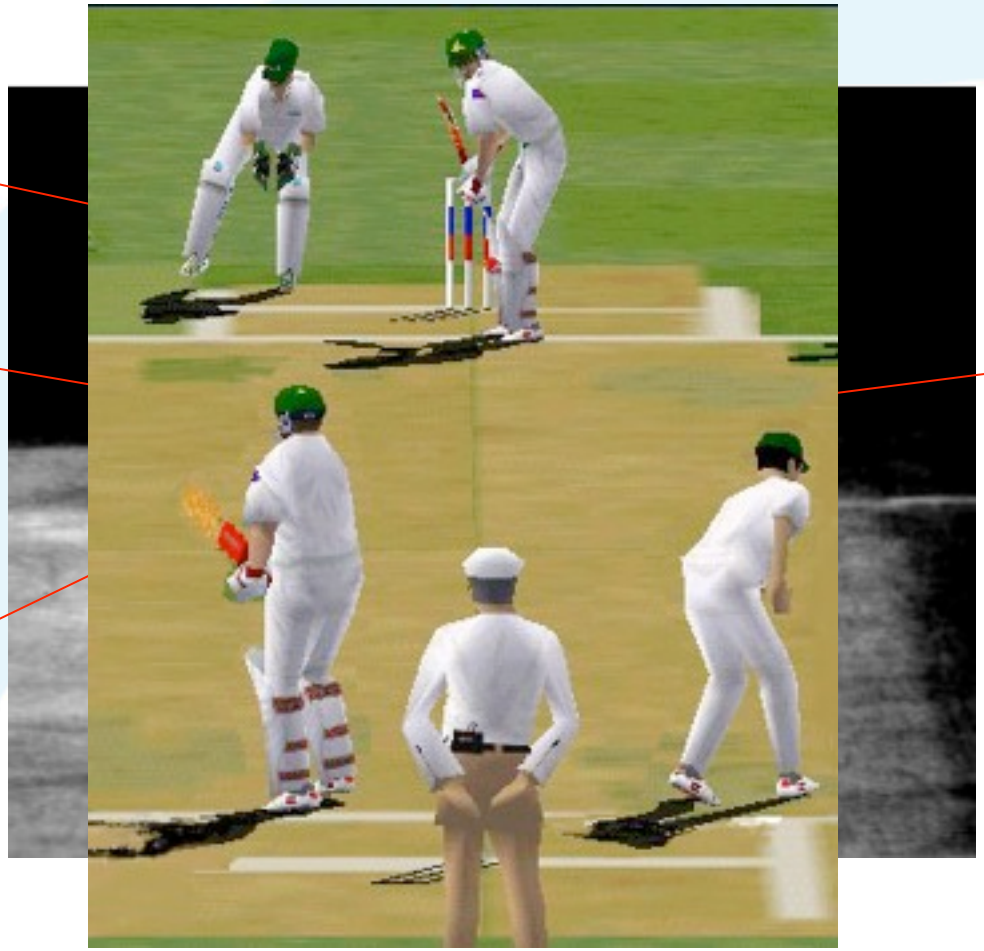

Thermal imagers at airports

Dienstag, 28. April 2009, 14:53 | update vor 5min

NILU

Thermography– the human body

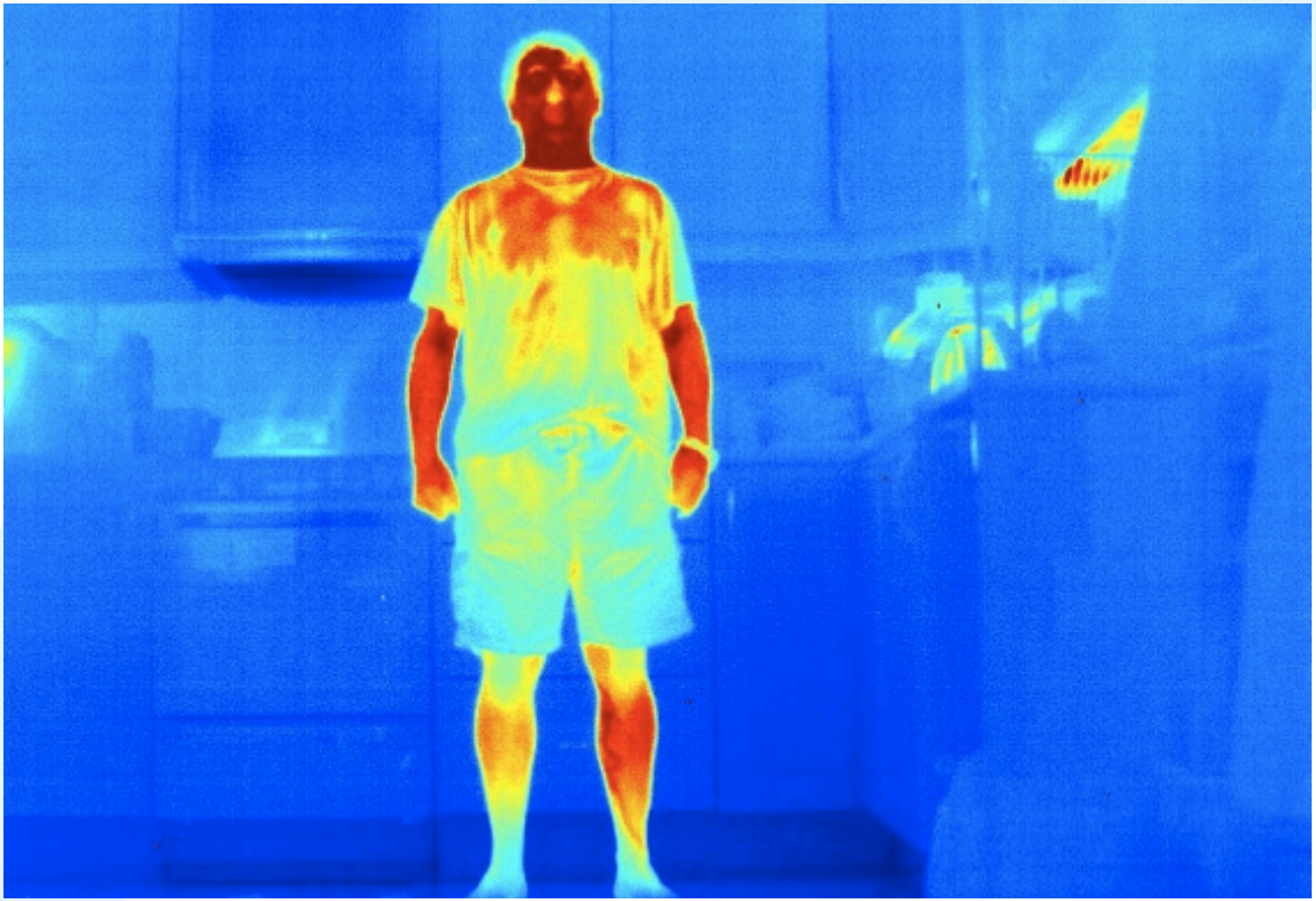

Body temperature

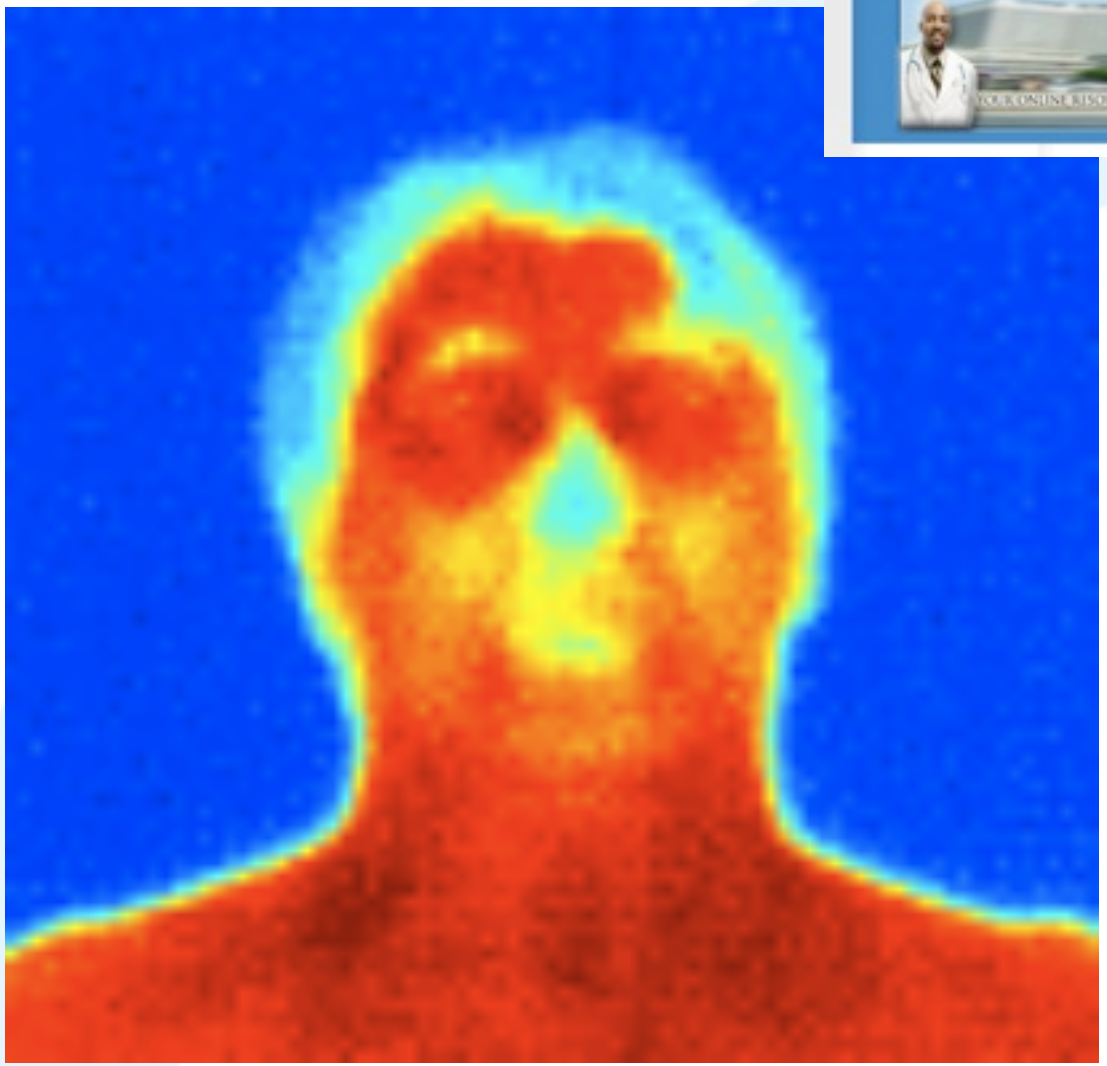

NILU

Newtonian cooling

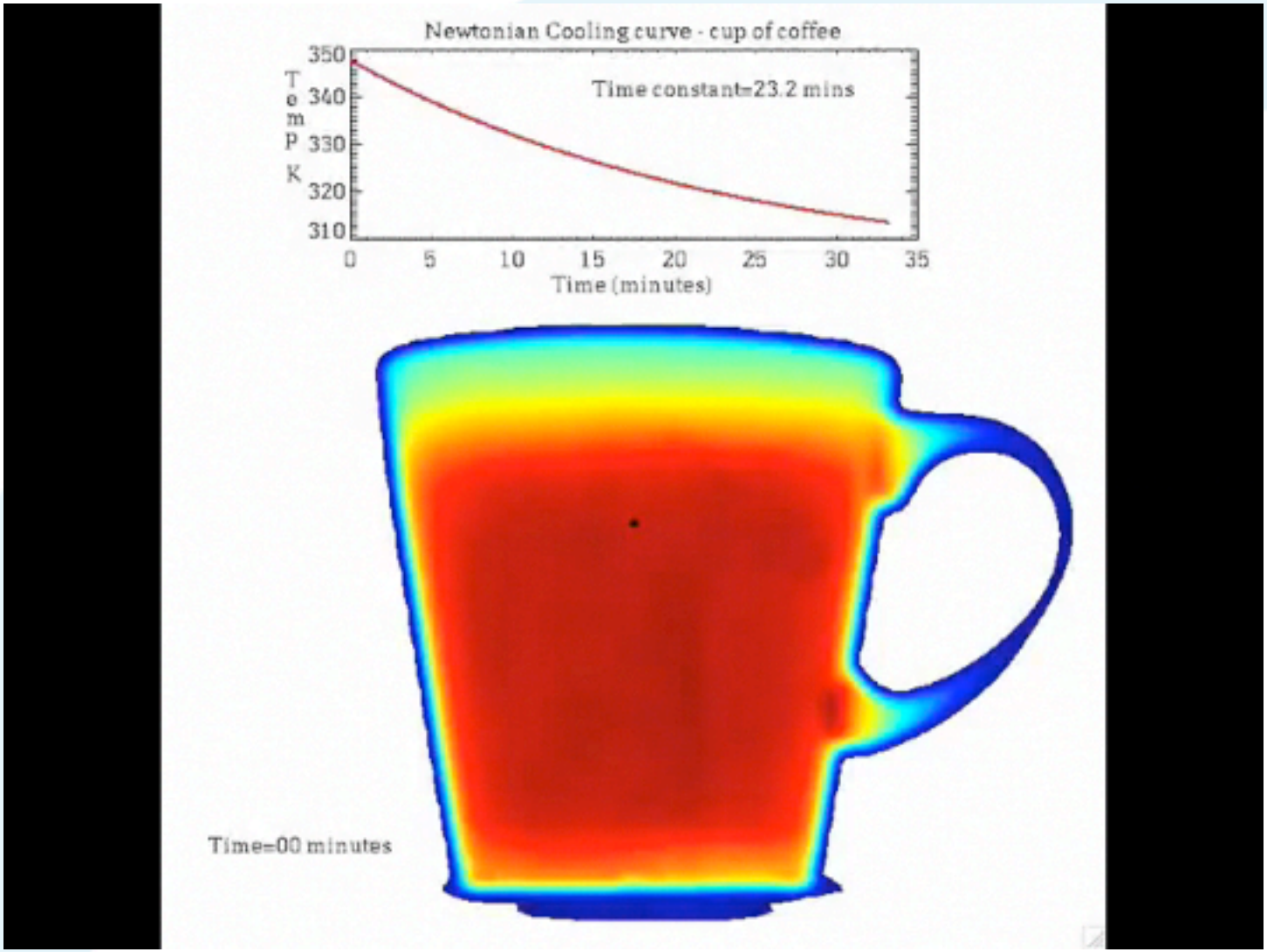

Vapour cooling

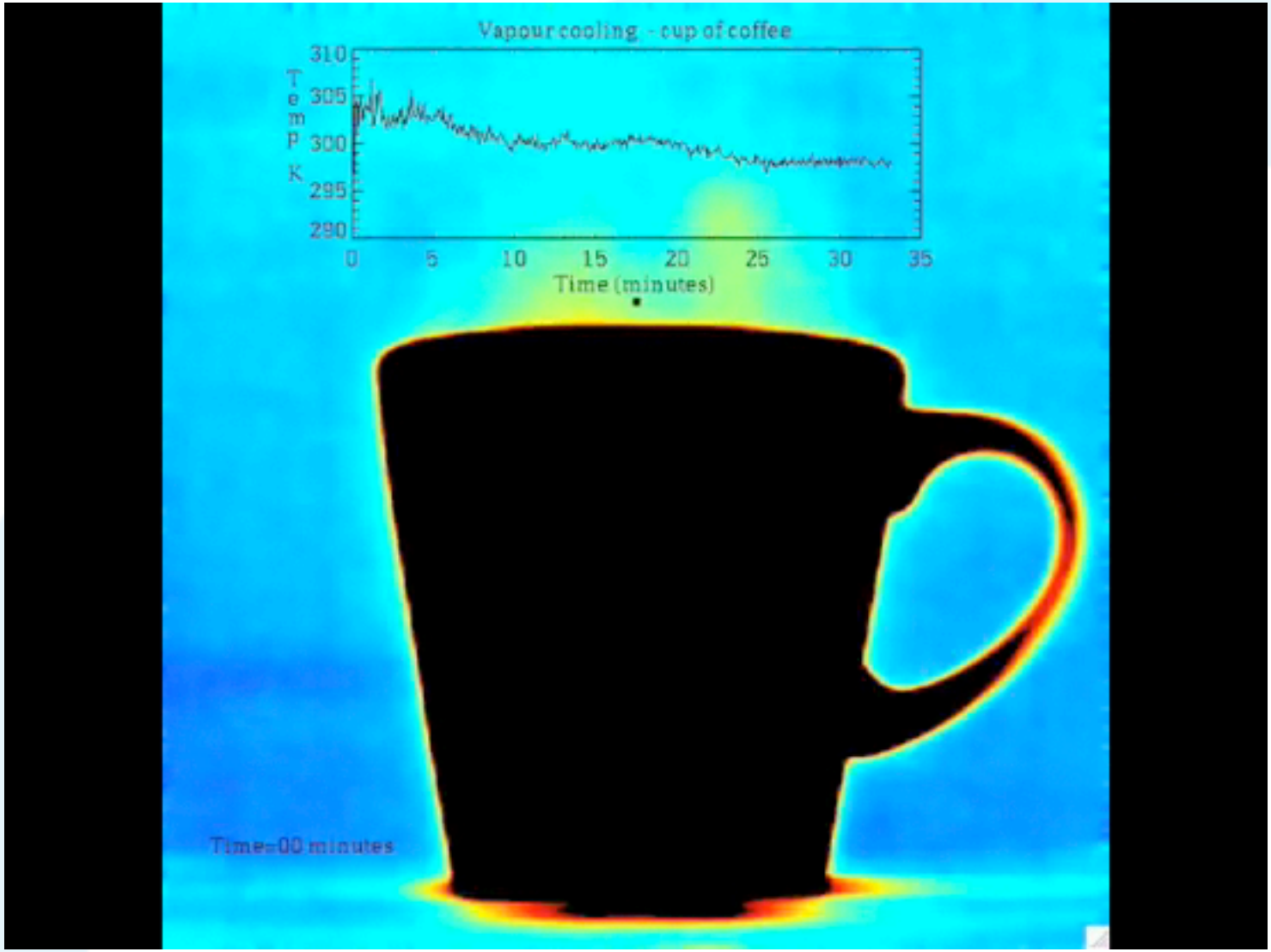

NicAIR – Imaging Camera

Dr Fred Prata

Senior Scientist

Climate and Atmosphere Department

Norwegian Institute for Air Research

Email: fred.prata@nilu.no

NILU Norsk institutt for luftforskning

Some theory -NEDT

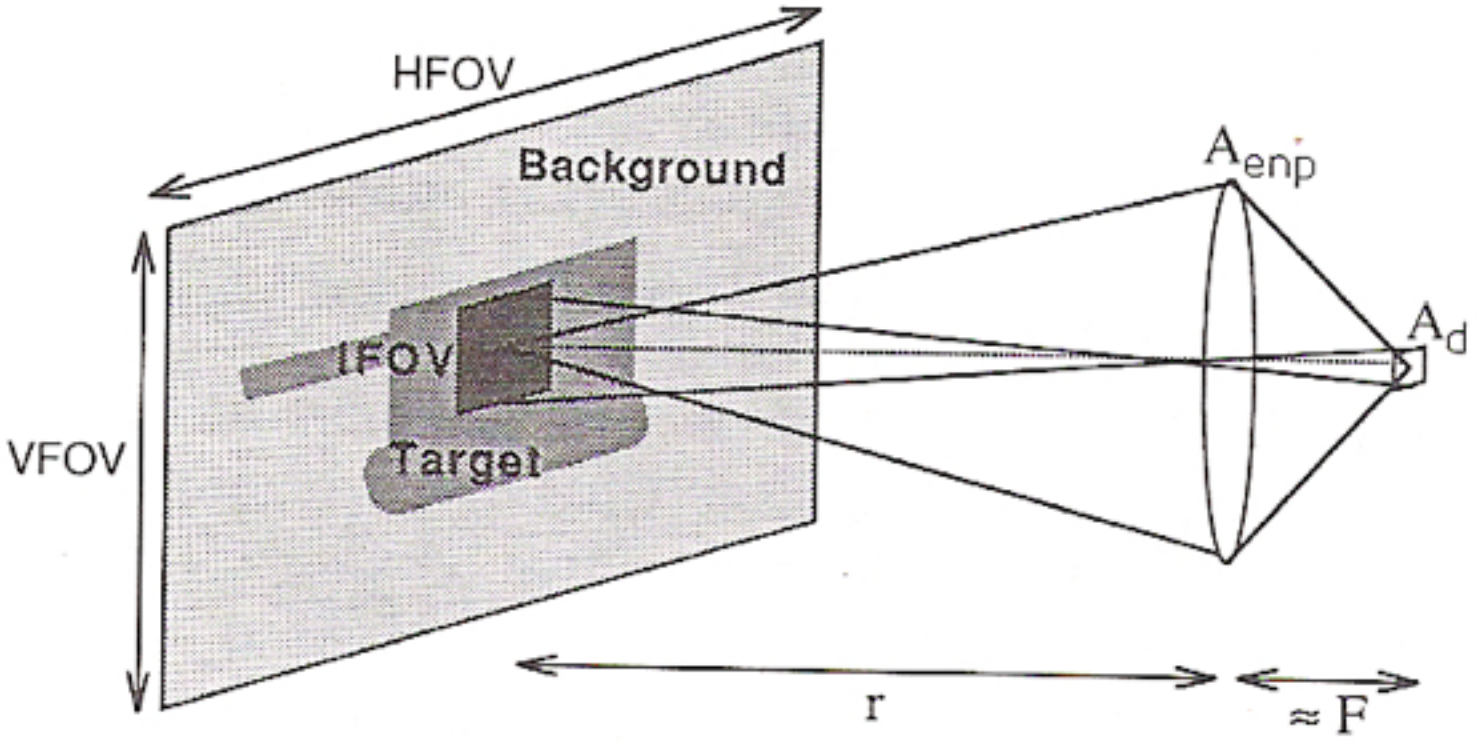

Flux	Φ	W
Radiance	L	W/(cm^2 sr)
Irradiance	E	W/cm^2

The flux (Φ) incident at the detector may be written:

$$\Phi_d = L \times A_{enp} \times \Omega_d \tag{1}$$

$$\Omega_d = \frac{A_d}{f} \tag{2}$$

$$A_{enp} = \frac{\pi}{4} D_{enp}^2 \tag{3}$$

$$\Phi = L \frac{\pi}{4} \frac{A_d}{(F\#)^2} \tag{4}$$

A_d = detector area

$F\#$= F-number (focal length/lens diameter)

NILU

The signal voltage (the detector counts after digitisation) is:

$$v_s = \mathcal{R}_v \times L \frac{\pi}{4} \frac{A_d}{(F\#)^2} \tag{5}$$

where $\mathcal{R}_v$ is the detector responsivity.

Since the system will have some wavelength dependence and some passband $\Delta\lambda$, the responsivity $\times$ the radiance is an integral over the passband:

$$\mathcal{R}_v \times L = \int_{\lambda_1}^{\lambda_2} \mathcal{R}_v(\lambda) L(\lambda) d\lambda. \tag{6}$$

The detector responds to a *change* in input radiance, generated by a *change* in temperature of the scene"

$$\frac{\Delta v_s}{\Delta T} = \mathcal{R}_v \times \frac{\partial L}{\partial T} \times \frac{\pi}{4} \frac{A_d}{(F\#)^2} \tag{7}$$

The detector response is:

$$\mathcal{R}_v = \frac{v_n}{NEP} \tag{8}$$

NILU

v_n is the noise voltage.

$$NEP = \frac{\sqrt{A_d}\sqrt{\Delta f}}{D^*} \tag{9}$$

$$SNR = \frac{v_s}{v_n} = \Delta T \times \frac{D^*}{\sqrt{\Delta f}} \times \frac{\partial L}{\partial T} \times \frac{\pi}{4} \frac{A_d}{(F\#)^2} \tag{10}$$

Set SNR=1 and solve for ΔT:

$$NE\Delta T = \frac{4}{\pi} \left[\frac{(F\#)^2 \sqrt{\Delta f}}{D^* \partial L / \partial T \sqrt{A_d}} \right] \tag{11}$$

NILU

Specifications

- <50 mK NEDT
- 50 Hz sampling
- 12-bit
- 320x240 microBolometer array
- Multi-filter
- Calibrated

NILU

Camera schematic

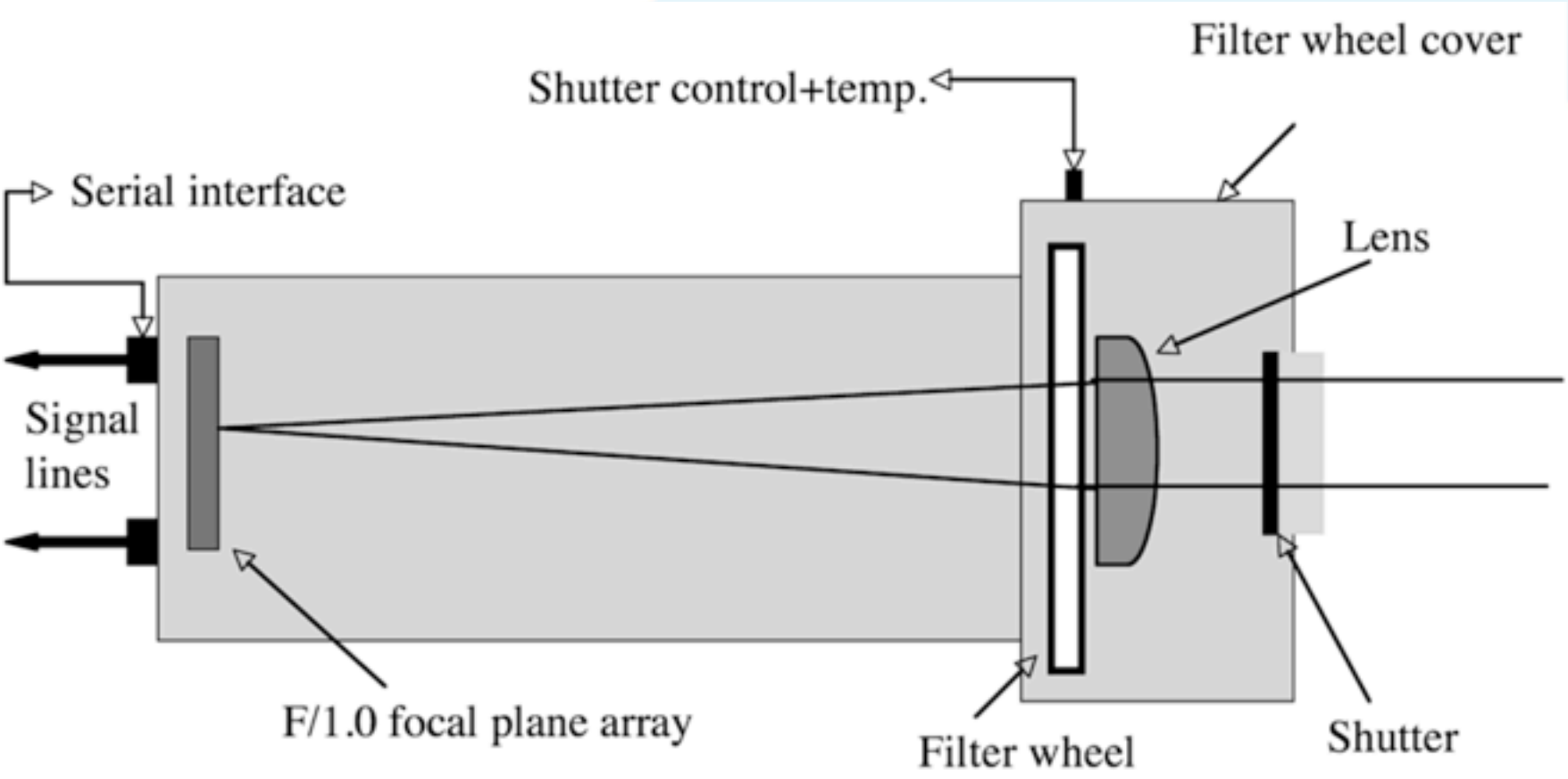

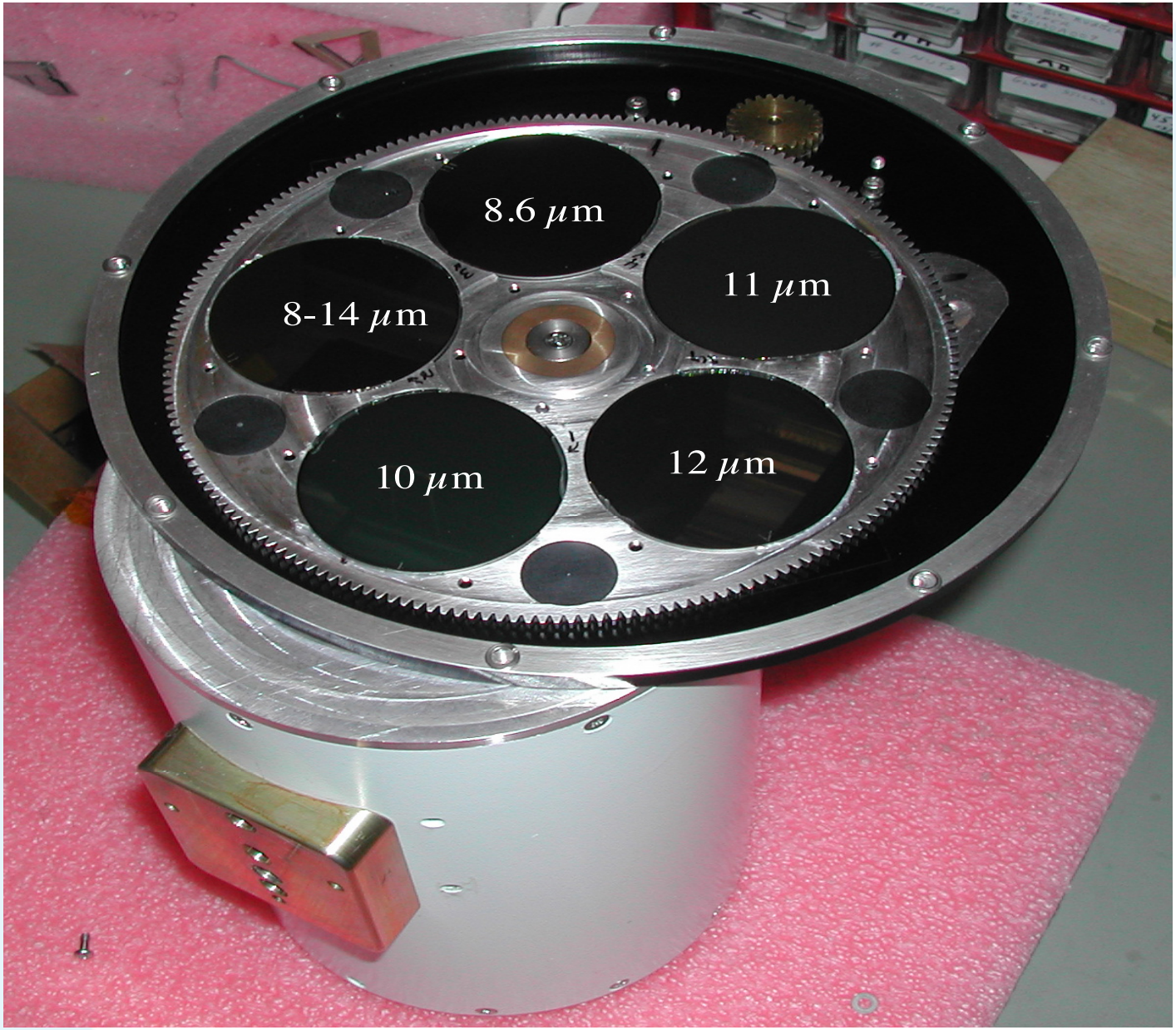

NILU

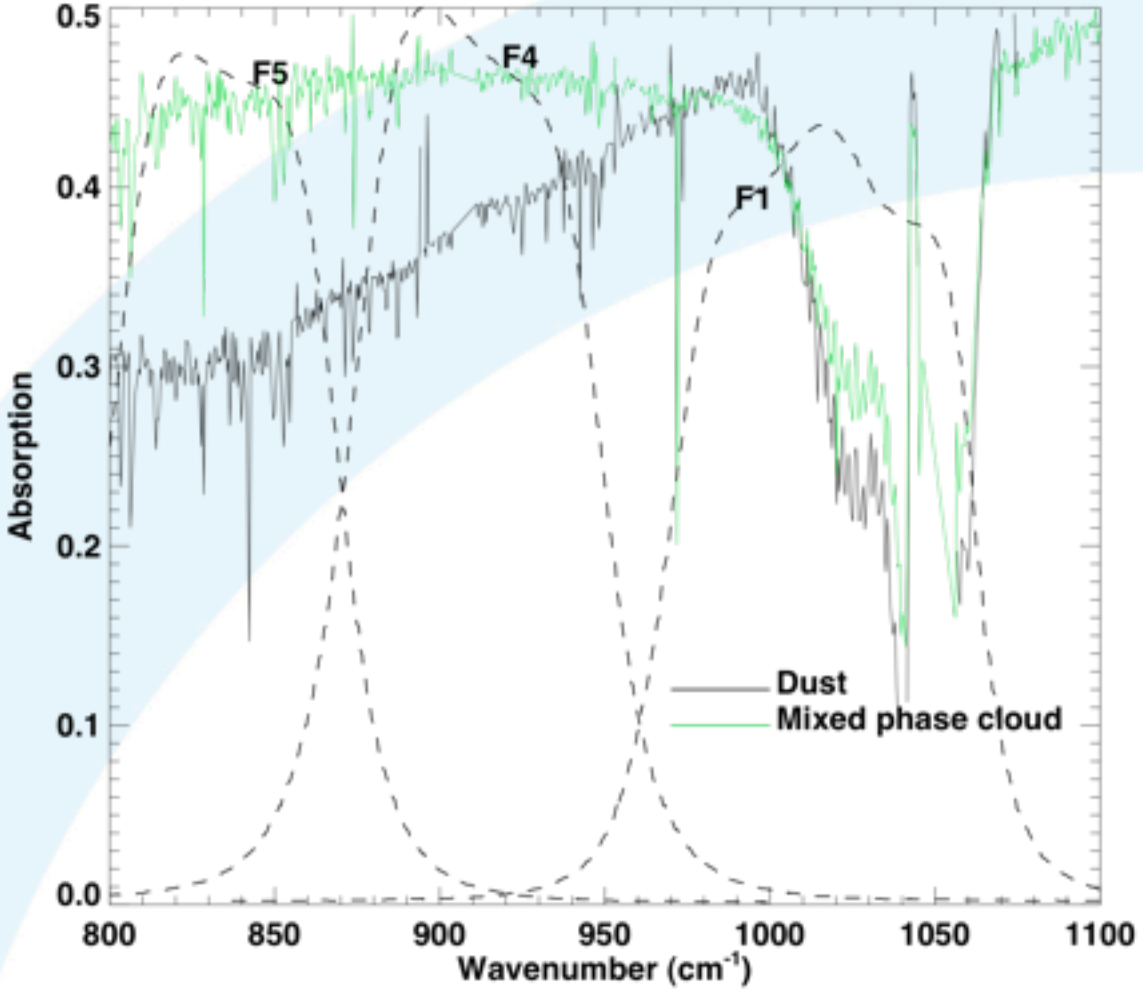
F5
F4
F1
Dust
Mixed phase cloud
Absorption
Wavenumber (cm-1)
0.0
0.1
0.2
0.3
0.4
0.5
800
850
900
950
1000
1050
1100

Horizontal Path Simulation (U.S. Std. Atmosphere)

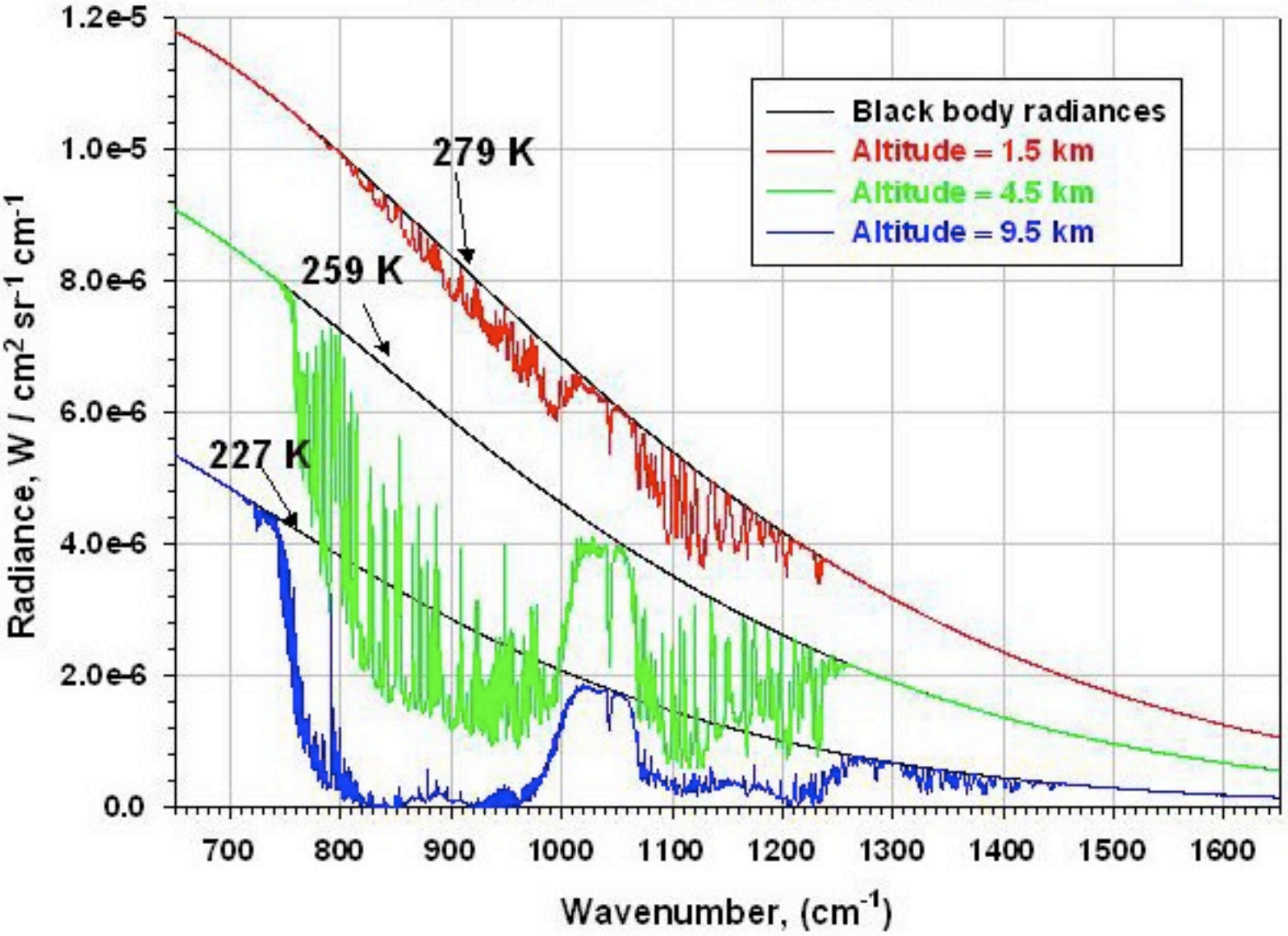

7.3 µm and 8.6 µm SO_2 bands

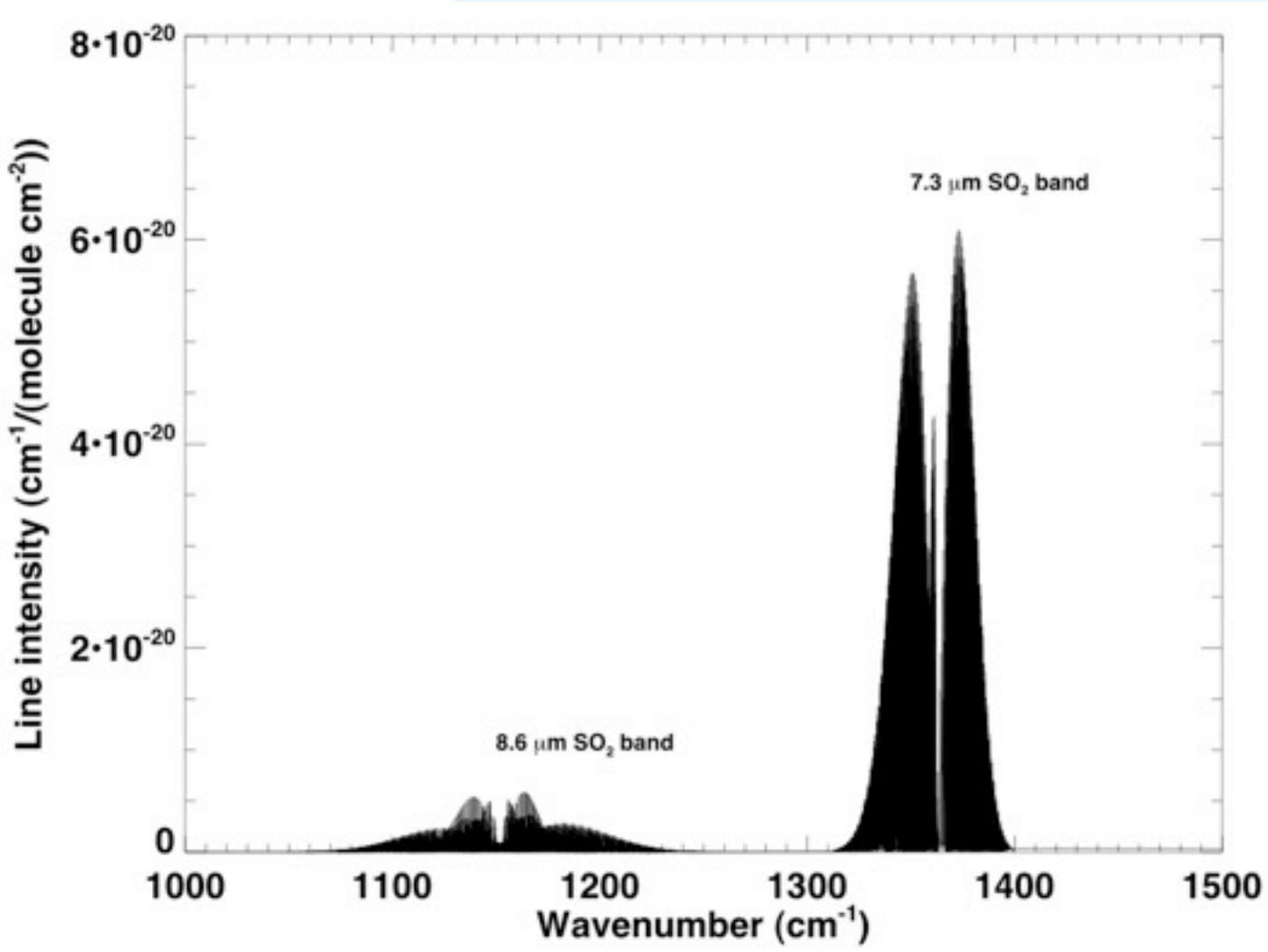

NILU

Broadband image

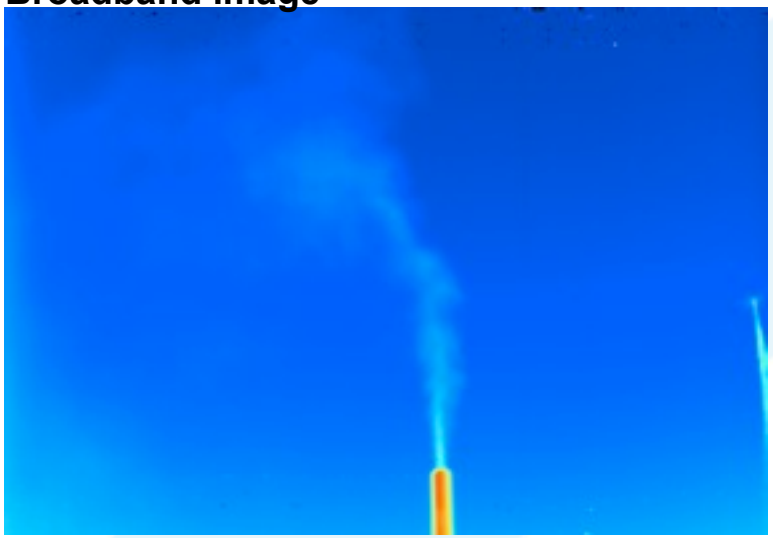

11 µm image

8.6 µm image

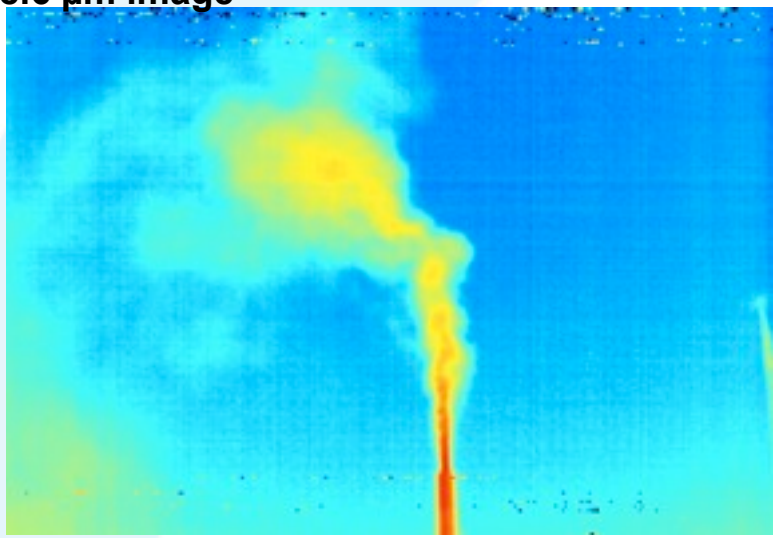

8.6-11 µm image (ΔTso_2)

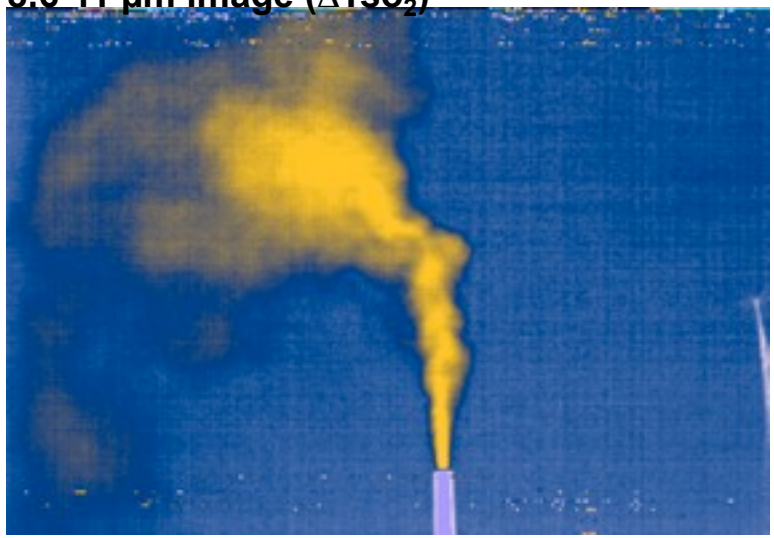

NILU

Ground-based Thermal IR SO_2 Measurements

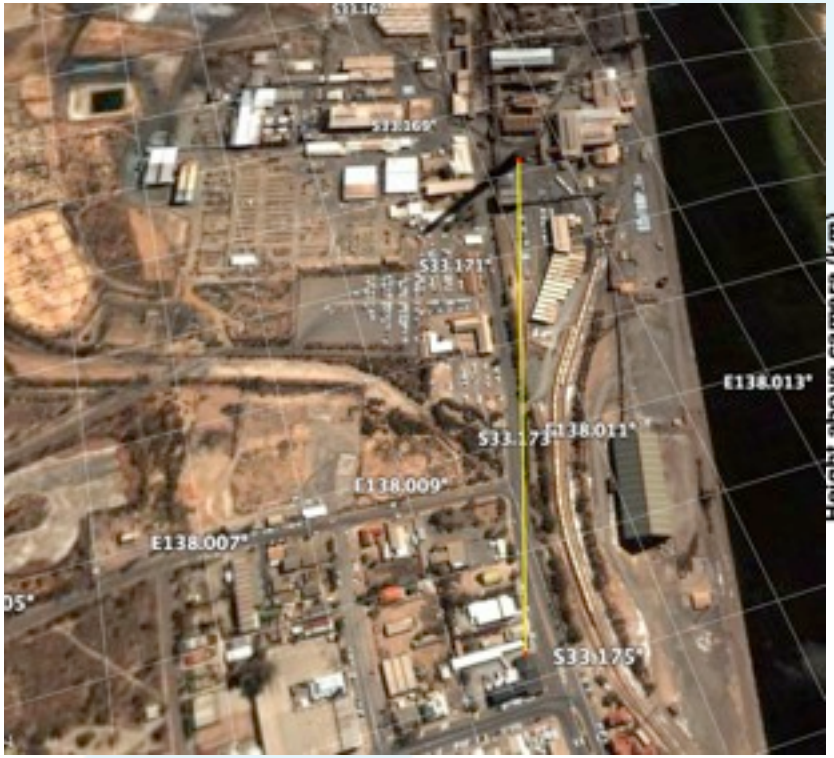

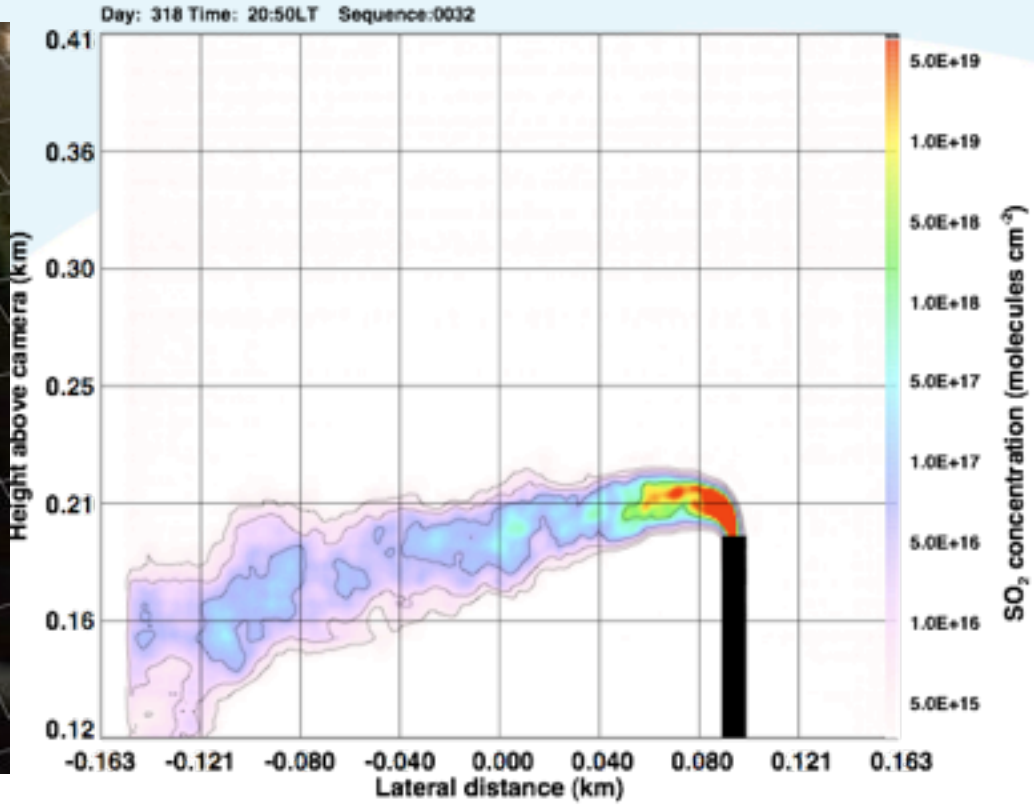

NILU

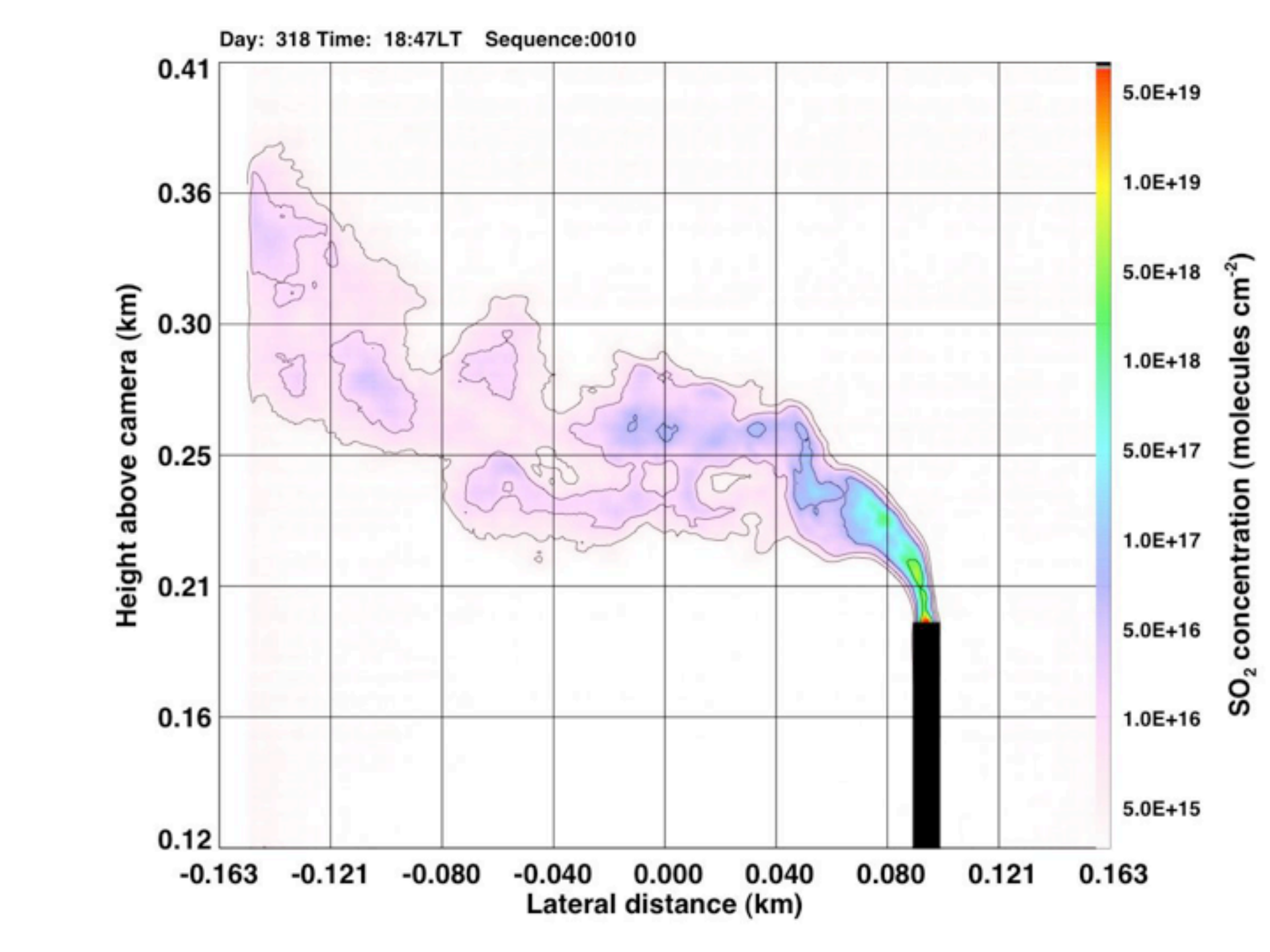
Day: 318 Time: 18:47LT Sequence:0010
Height above camera (km)
0.41
0.36
0.30
0.25
0.21
0.16
0.12
-0.163
-0.121
-0.080
-0.040
0.000
0.040
0.080
0.121
0.163
Lateral distance (km)
5.0E+19
1.0E+19
5.0E+18
1.0E+18
5.0E+17
1.0E+17
5.0E+16
1.0E+16
5.0E+15
SO2 concentration (molecules cm-2)

SO_2 and H_2O at Etna

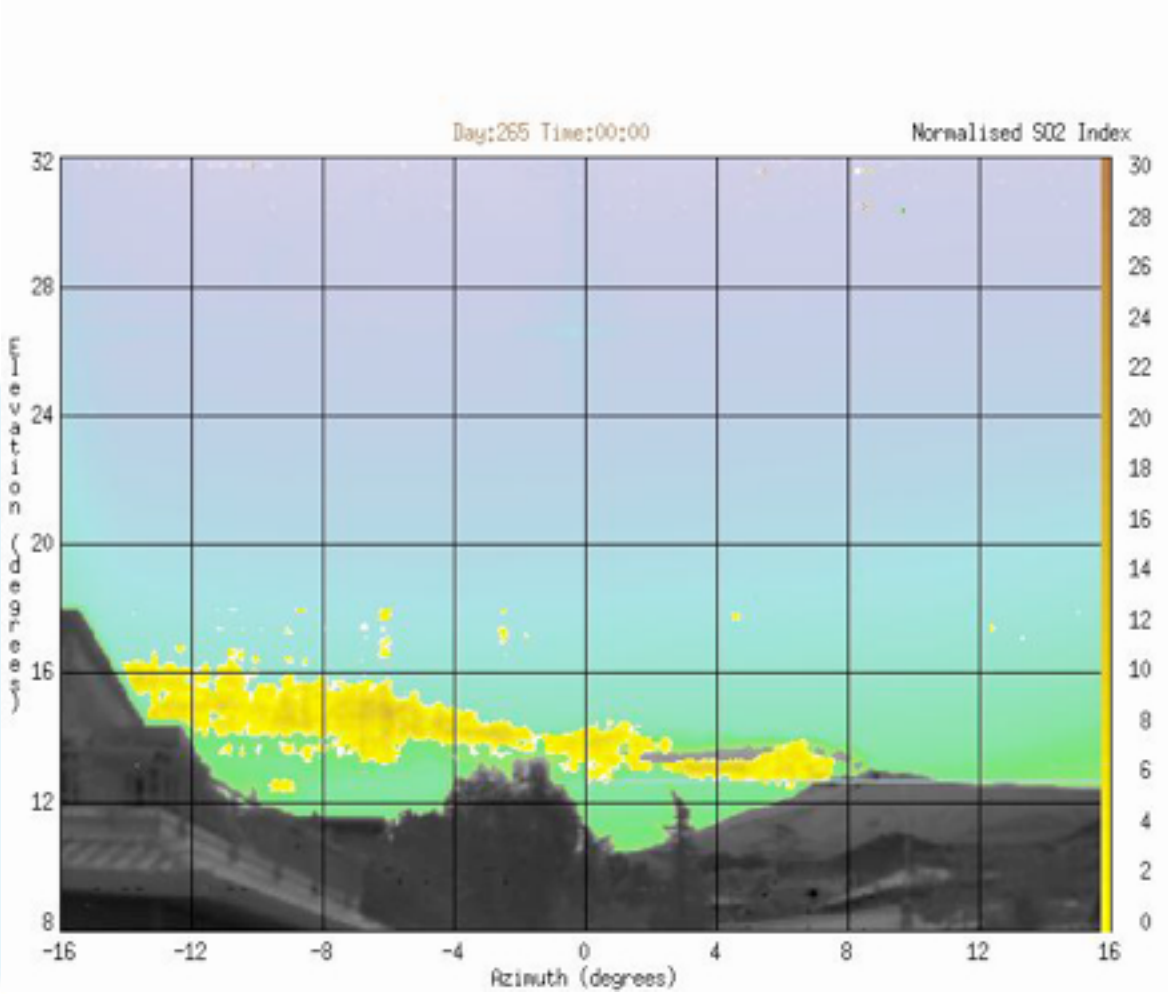

NILU

Stromboli

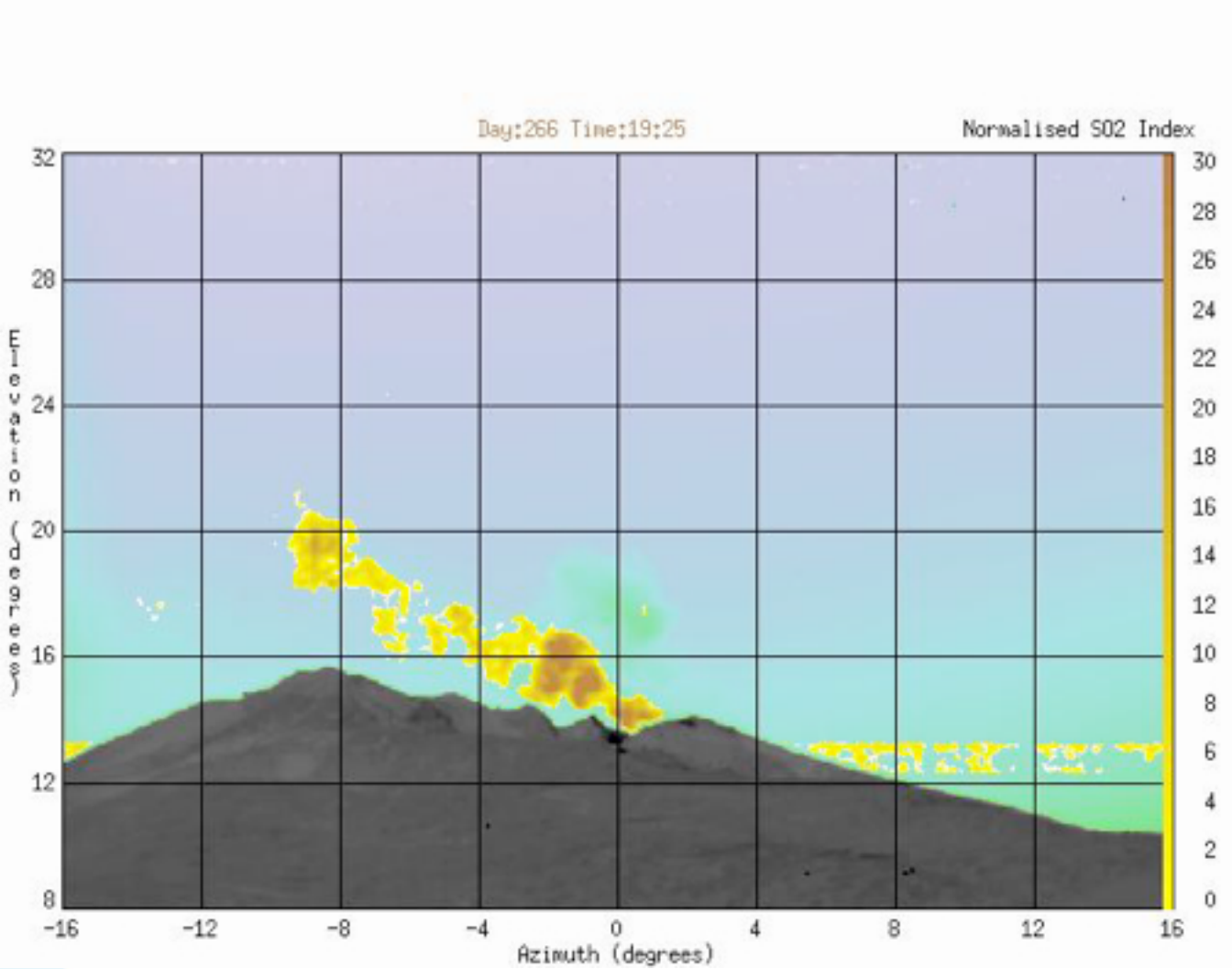
Day:266 Time:19:25
Normalised SO2 Index
Elevation (degrees)
32
28
24
20
16
12
8
30
28
26
24
22
20
18
16
14
12
10
8
6
4
2
0
-16
-12
-8
-4
0
4
8
12
16
Azimuth (degrees)

Etna volcano

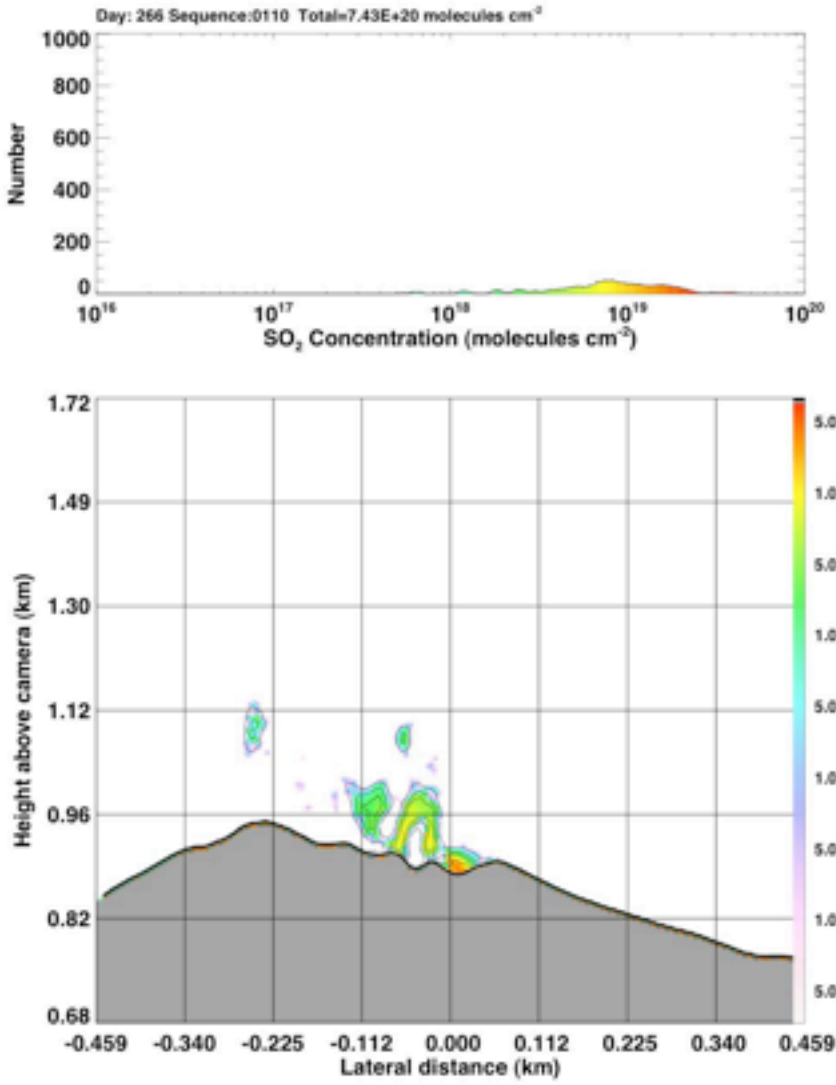

Model for SO_2 Retrieval

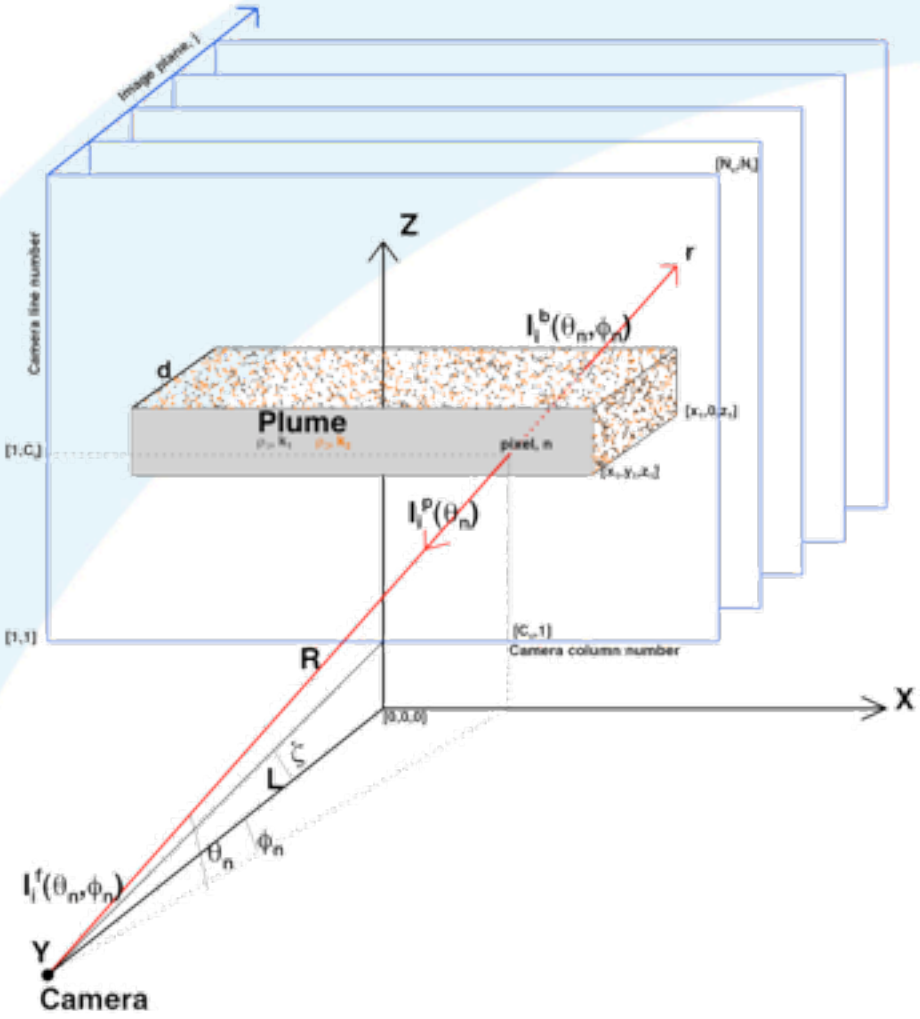

NILU

The radiation received at the imager may be written:

$$I_i(\theta) = I_i^f(\theta,\phi) + I_i^p(\theta,\phi) + I_i^b(\theta,\phi)$$

θ zenith angle

ϕ azimuth angle

$$m^* = \rho d = -\frac{1}{k}\cos\theta\cos\phi\ln[1-\epsilon]$$

$$\epsilon = \frac{(\Delta T_{i,j}^p - \Delta T_{i,j}^o) - \Delta T_i^p(1 - \Delta T_{p,j}/\Delta T_{p,i})}{\Delta T_{p,j}(1 - \Delta T_i^p/\Delta T_{p,i})}$$

NILU

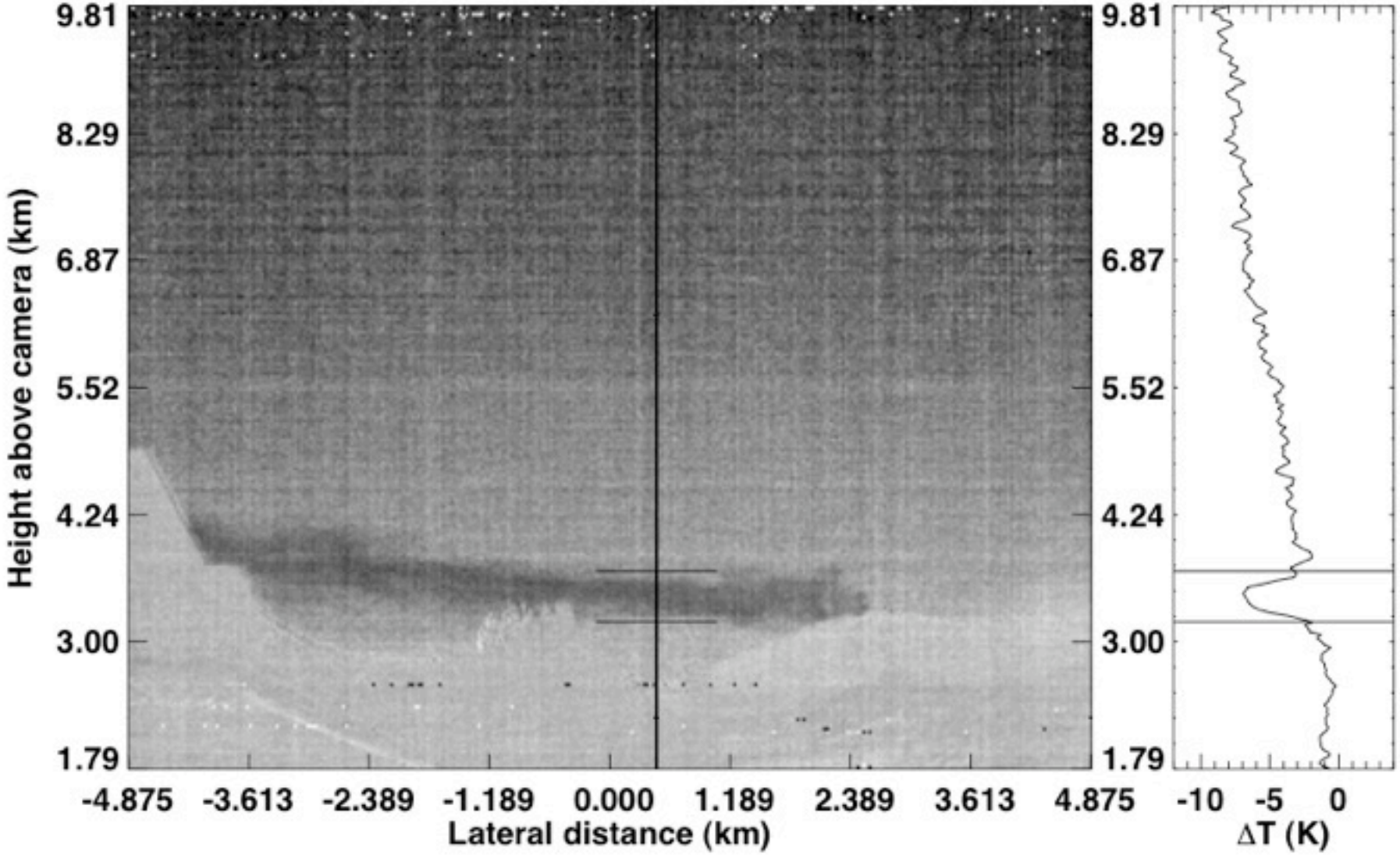
9.81
8.29
6.87
5.52
4.24
3.00
1.79
Height above camera (km)
-4.875
-3.613
-2.389
-1.189
0.000
1.189
2.389
3.613
4.875
Lateral distance (km)
-10
-5
0
ΔT (K)

NILU

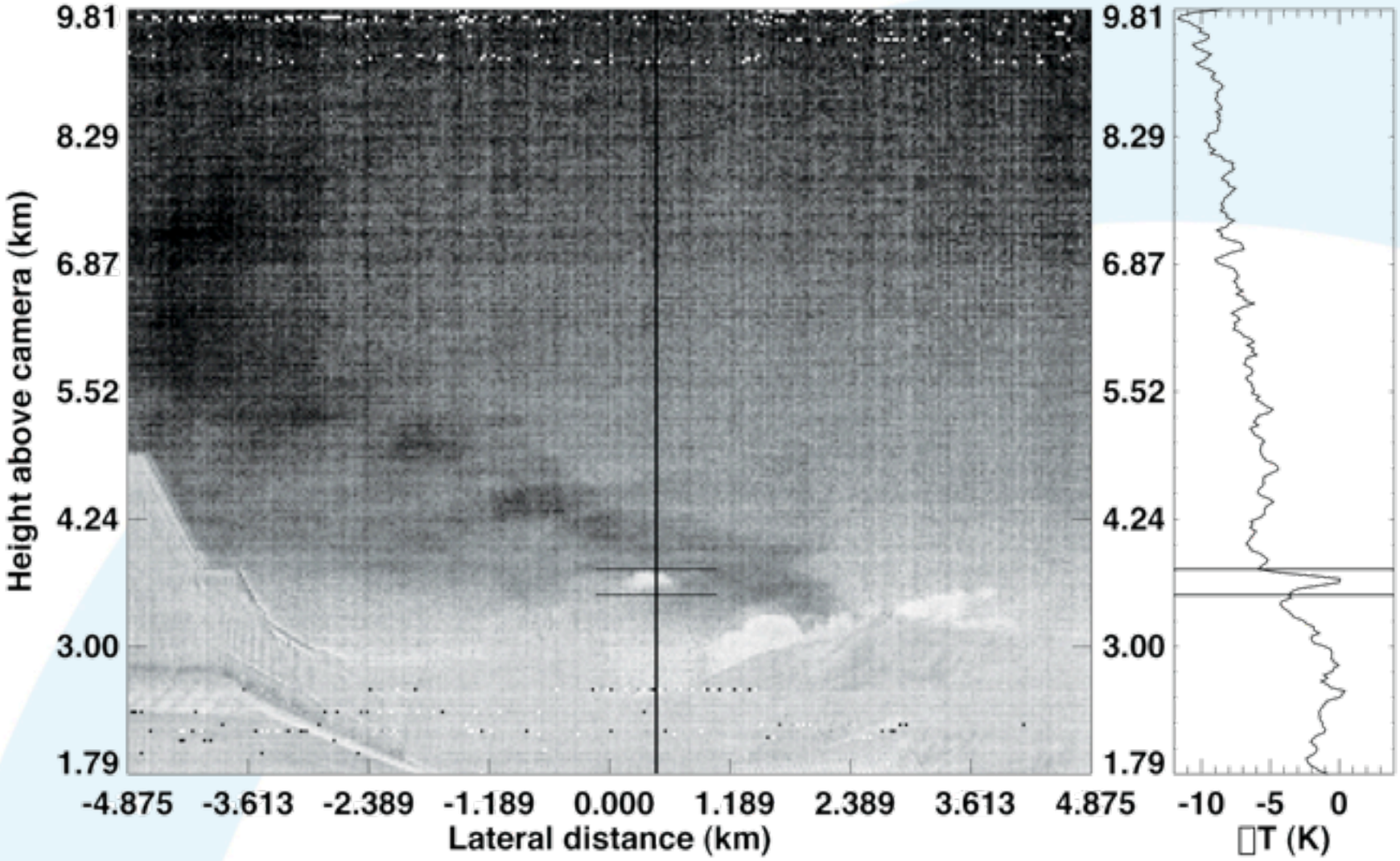
9.81
8.29
6.87
5.52
4.24
3.00
1.79
Height above camera (km)
-4.875
-3.613
-2.389
-1.189
0.000
1.189
2.389
3.613
4.875
Lateral distance (km)
-10
-5
0
T (K)

NILU

Temperature differences

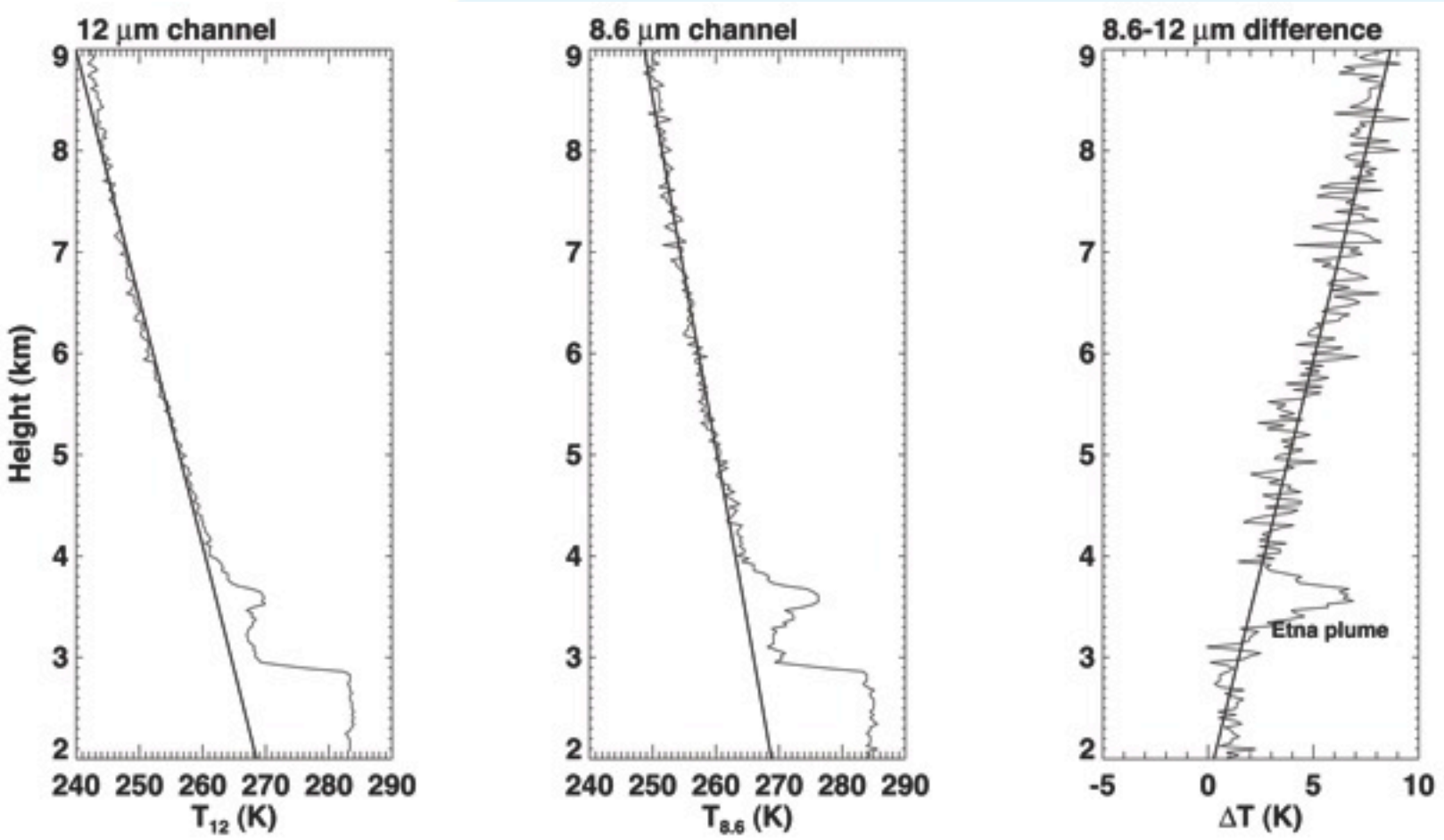

NILU

(a) Broadband

(b) 12 μm channel

(c) 11 μm channel

(d) 8.6 μm channel

(e) 10 μm channel

(f) SO_2 retrieval

NILU

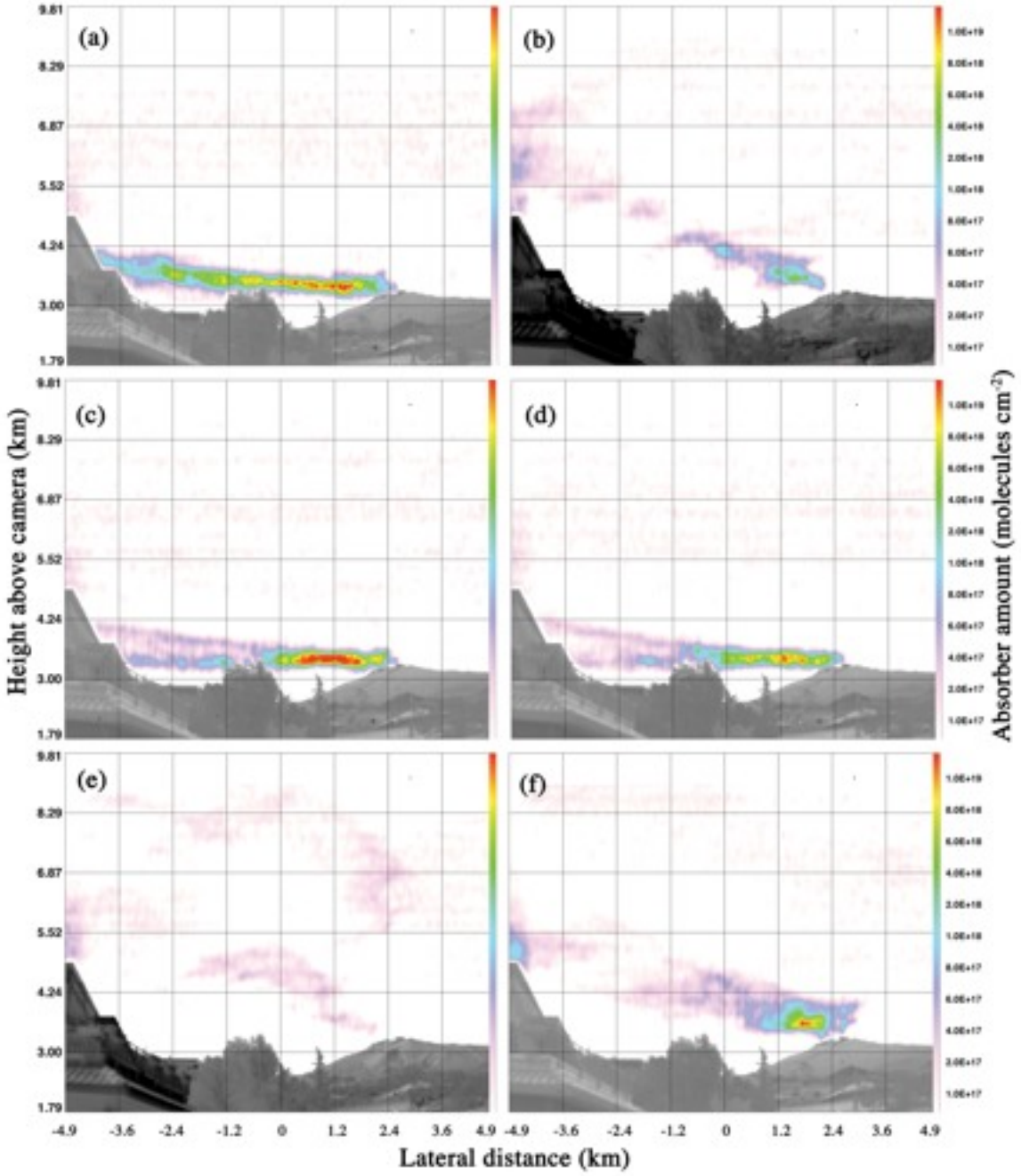
(a)
(b)
(c)
(d)
(e)
(f)
Height above camera (km)
9.81
8.29
6.87
5.52
4.24
3.00
1.79
-4.9
-3.6
-2.4
-1.2
0
1.2
2.4
3.6
4.9
Lateral distance (km)
Absorber amount (molecules cm-2)

NILU

Measurements at Anatahan Volcano

NILU

Ground-based measurements in Rabaul, New Britain, PNG

"*The Research Team*"

NILU

Tavurvur, New Britain

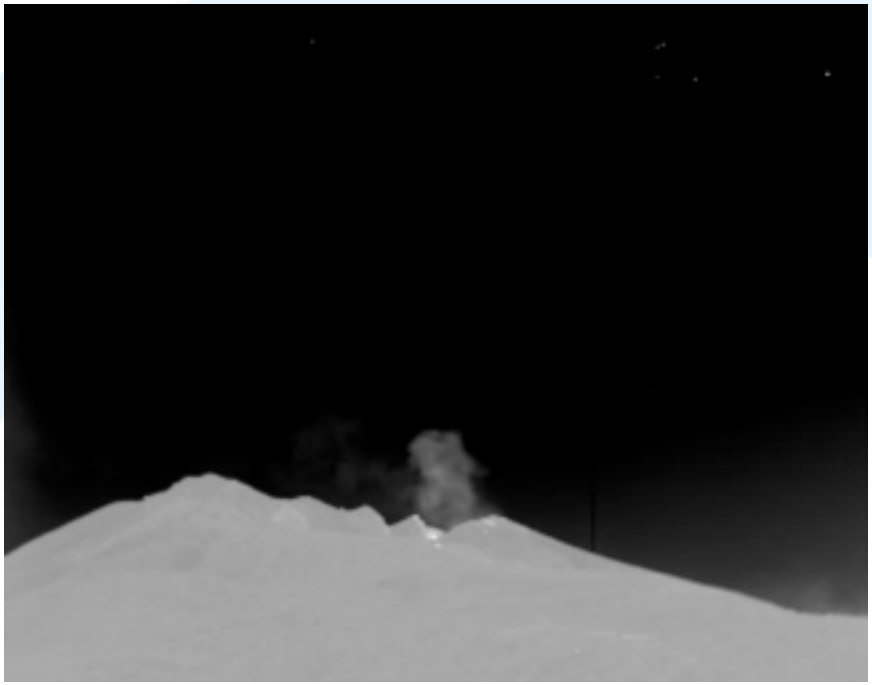

Stromboli (Italy)

NILU

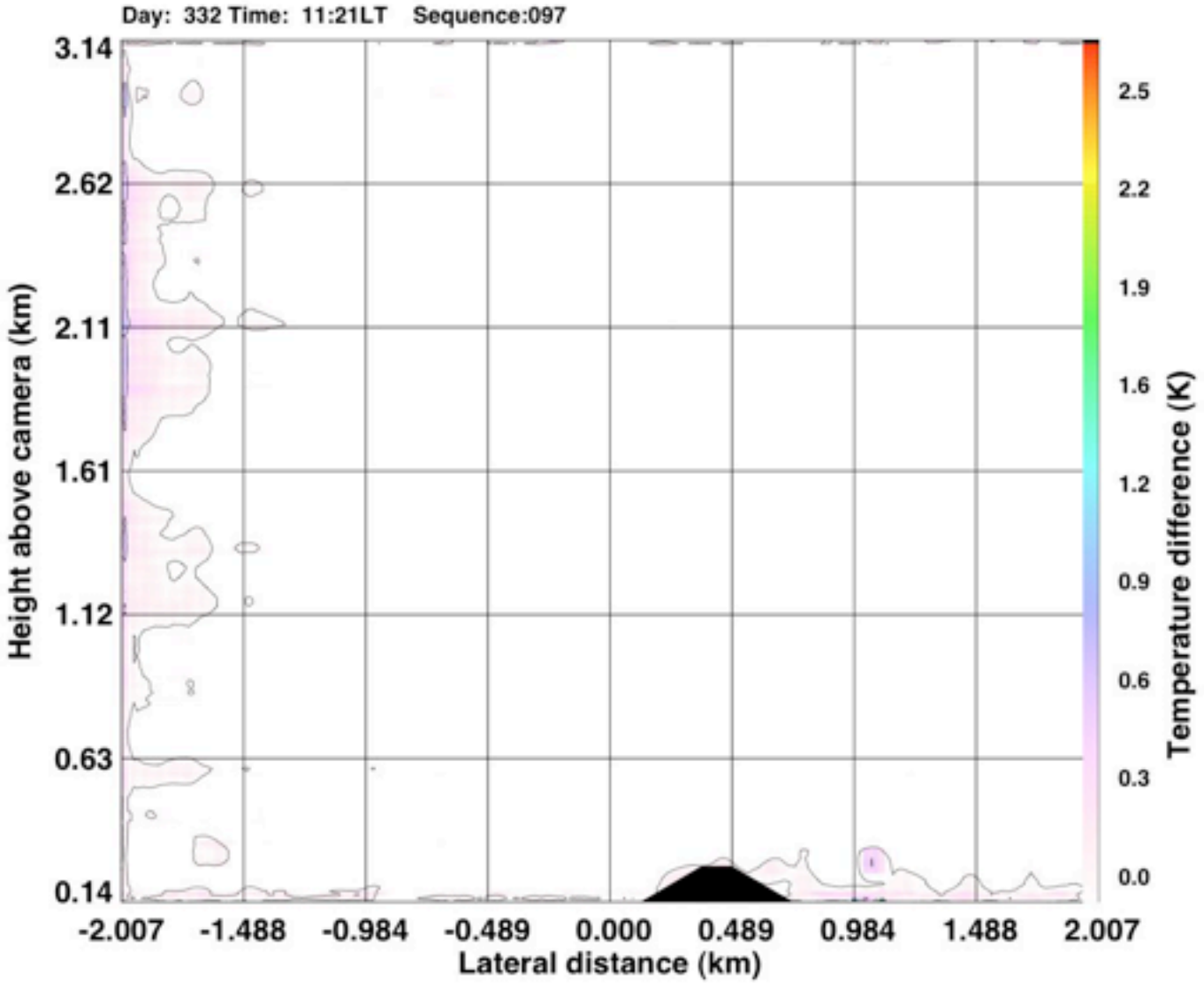
Day: 332 Time: 11:21LT Sequence:097
Height above camera (km)
3.14
2.62
2.11
1.61
1.12
0.63
0.14
-2.007
-1.488
-0.984
-0.489
0.000
0.489
0.984
1.488
2.007
Lateral distance (km)
Temperature difference (K)
2.5
2.2
1.9
1.6
1.2
0.9
0.6
0.3
0.0

NILU

Teperature differences can be related to particle microphysical properties

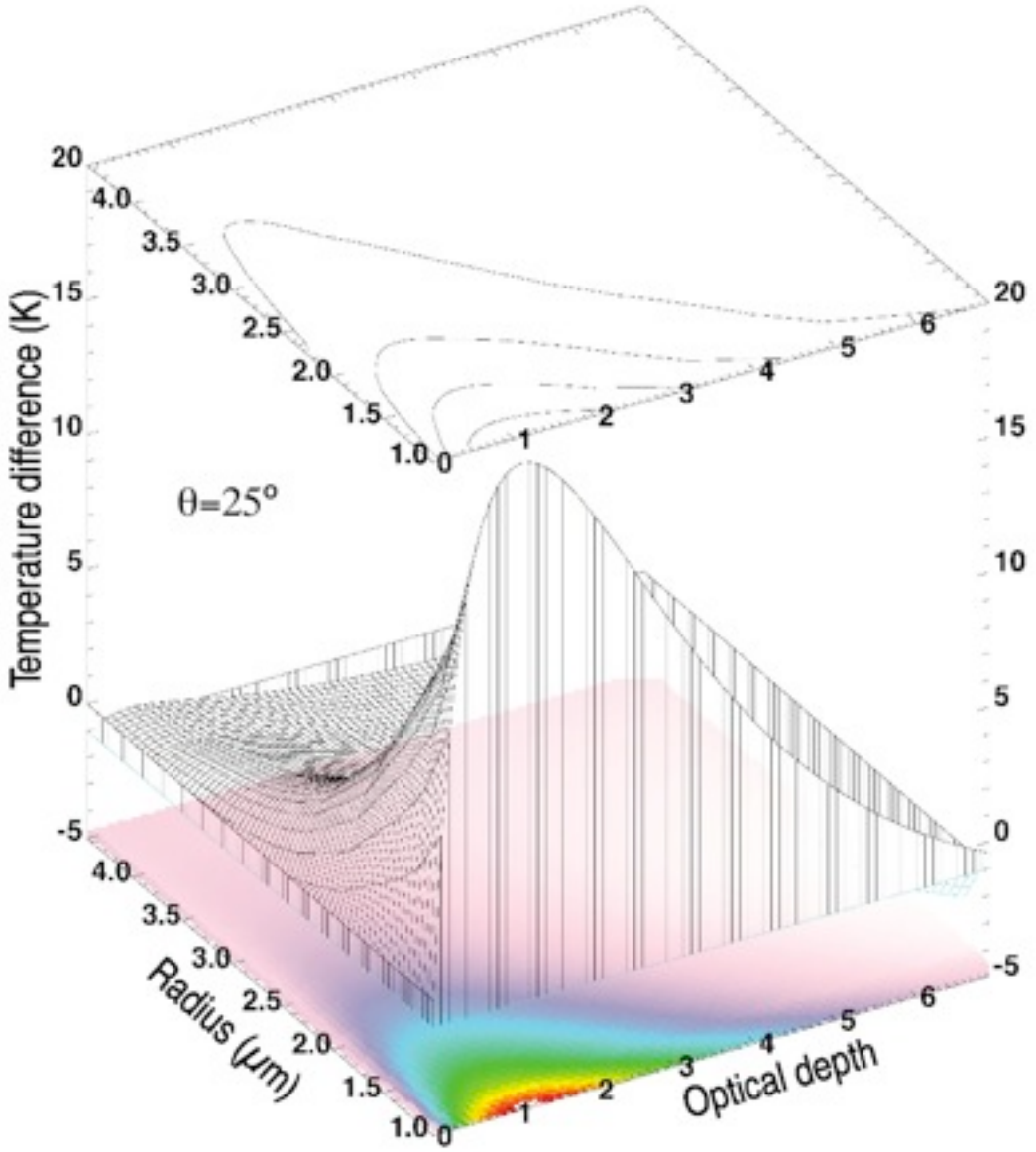

NILU

Retrieval scheme

$$I(\theta, z_t, \nu) = \int_{p(0)}^{p(z_t)} B[T(p), \nu] \frac{\partial \tau(\theta, p, \nu)}{\partial p} dp \quad 0 \leq \theta \leq 85.$$

$$\mathcal{R}(r, \tau, \theta; M) \leftarrow \mathcal{G}(T_i, \Delta T_{i,j}, \theta; P).$$

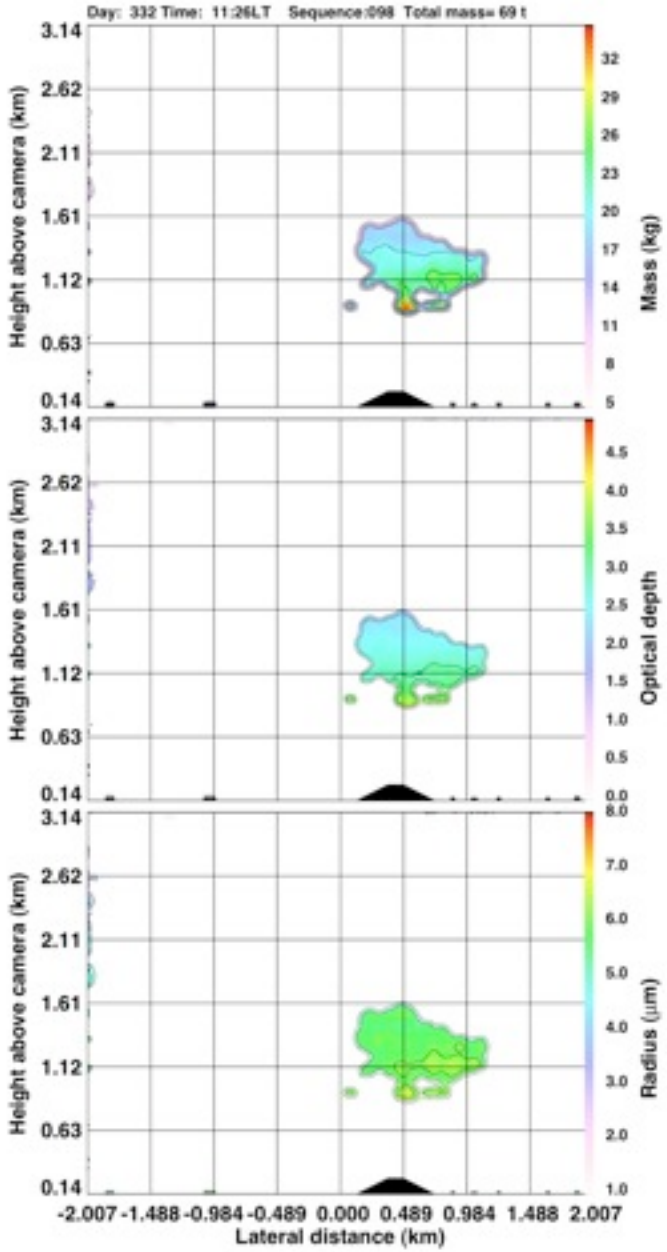

CyClops

NILU

CyClops

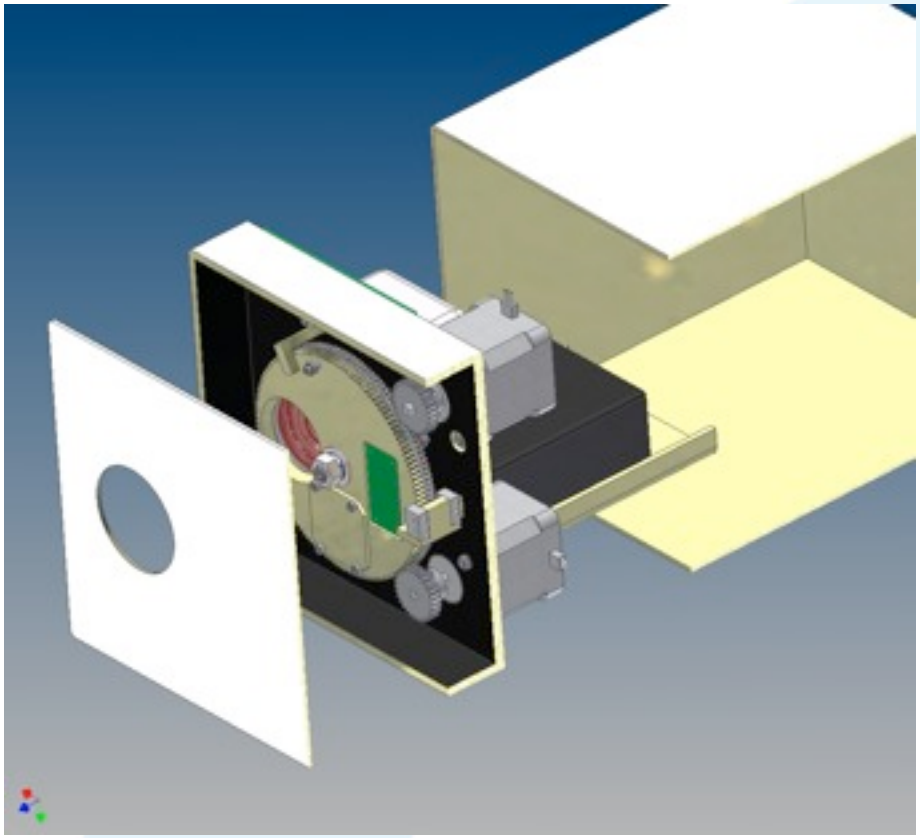

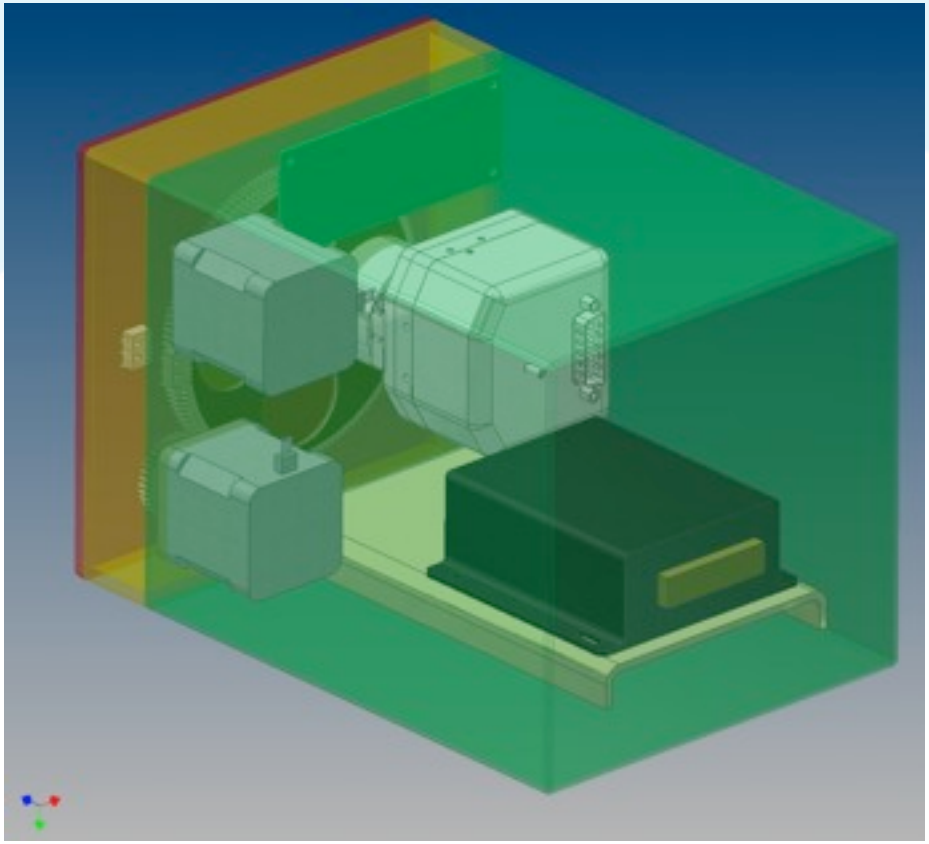

NILU

NicAIR
(was CyClops)

NILU

Sky measurments

Clear sky

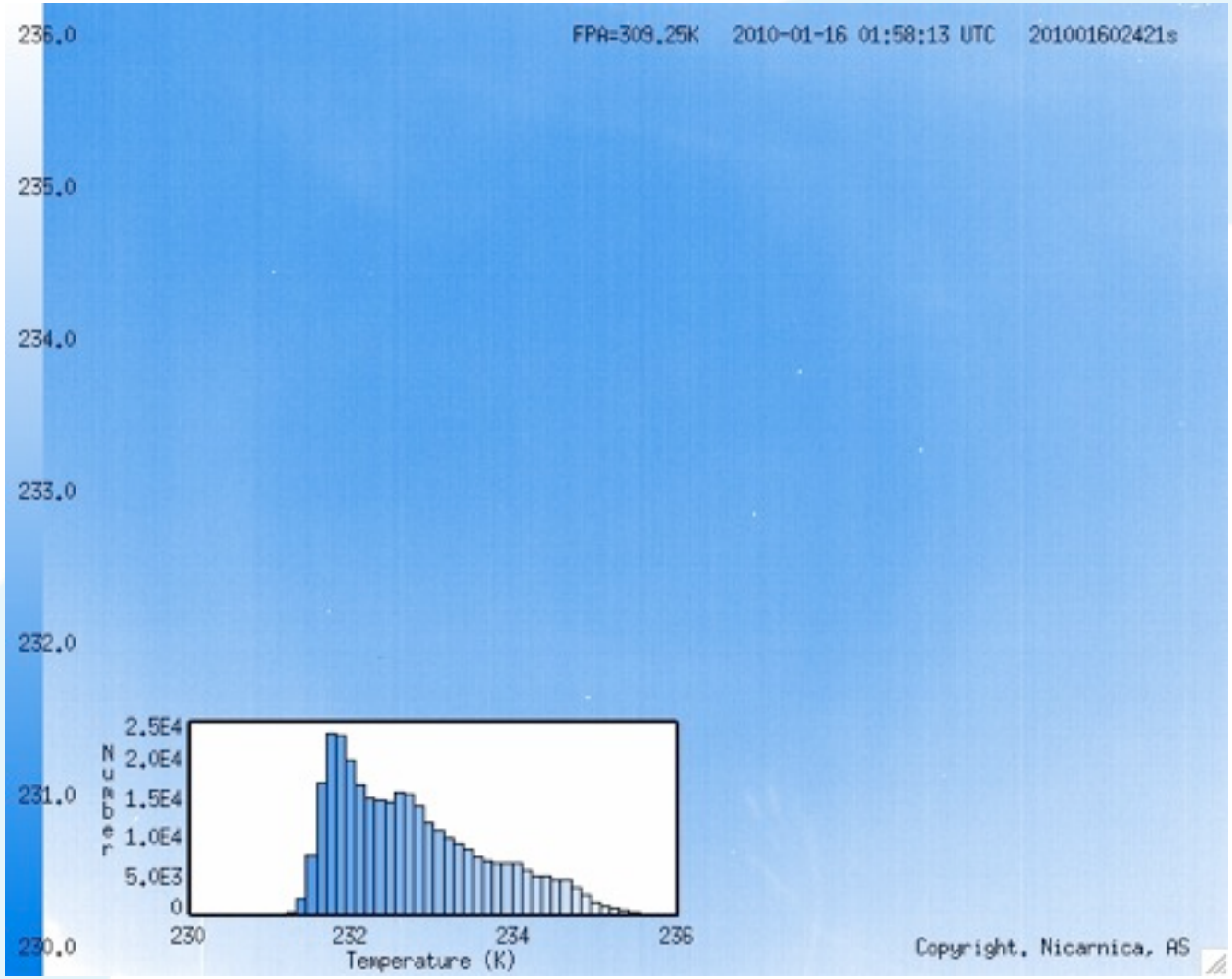
FPA=309.25K 2010-01-16 01:58:13 UTC 201001602421s
236.0
235.0
234.0
233.0
232.0
231.0
230.0
2.5E4
2.0E4
1.5E4
1.0E4
5.0E3
0
Number
230
232
234
236
Temperature (K)
Copyright, Nicarnica, AS

Sky, clouds, trees

Sky, clouds, trees

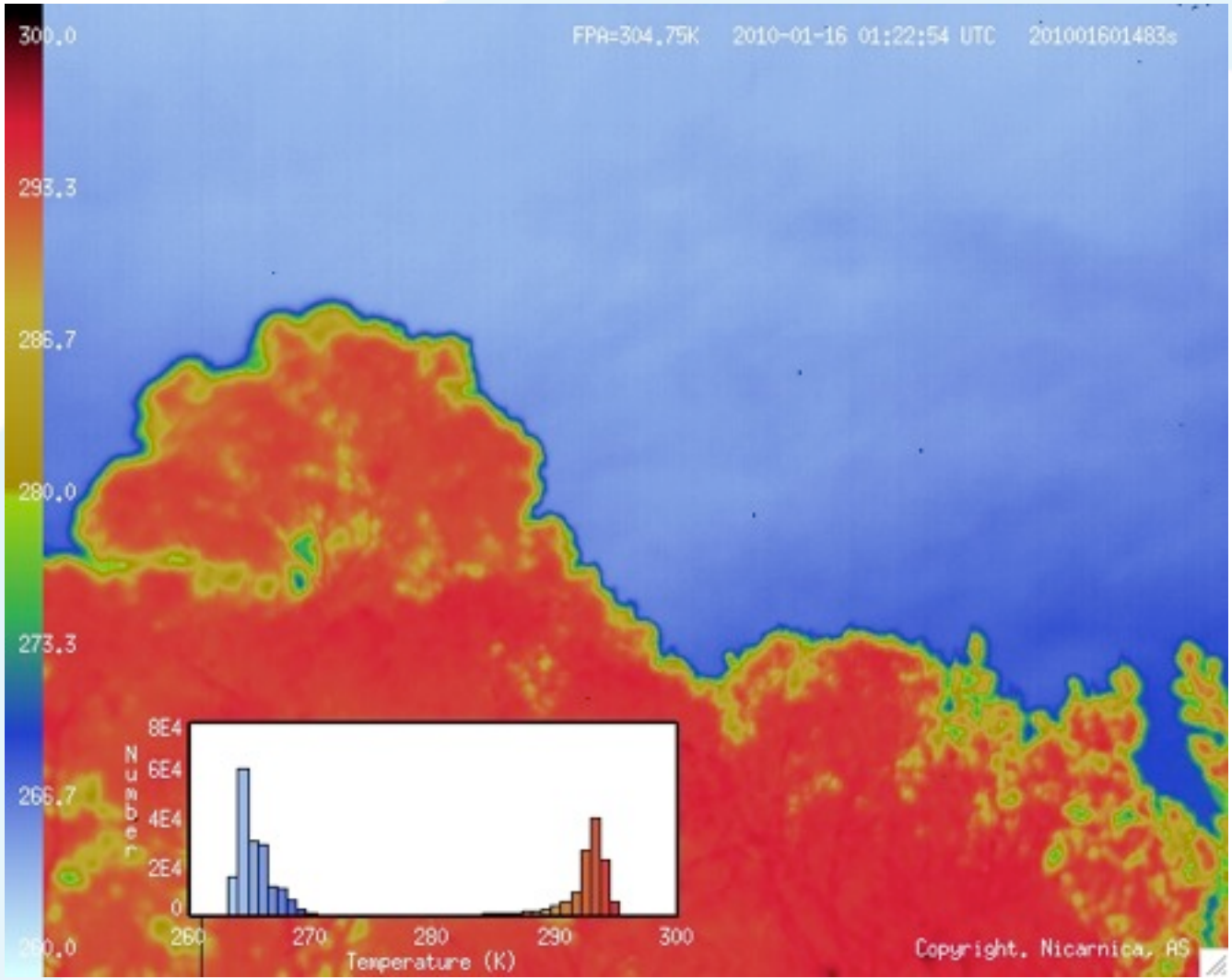

NILU

Camera viewing water/wood/tile


FPA=306.35K 2010-01-16 02:19:00 UTC 201001602914s
320.0
315.0
310.0
305.0
300.0
295.0
290.0
1E5
8E4
6E4
4E4
2E4
0
Number
290
300
310
320
Temperature (K)
Copyright. Nicarnica. AS

NILU

Measurement example

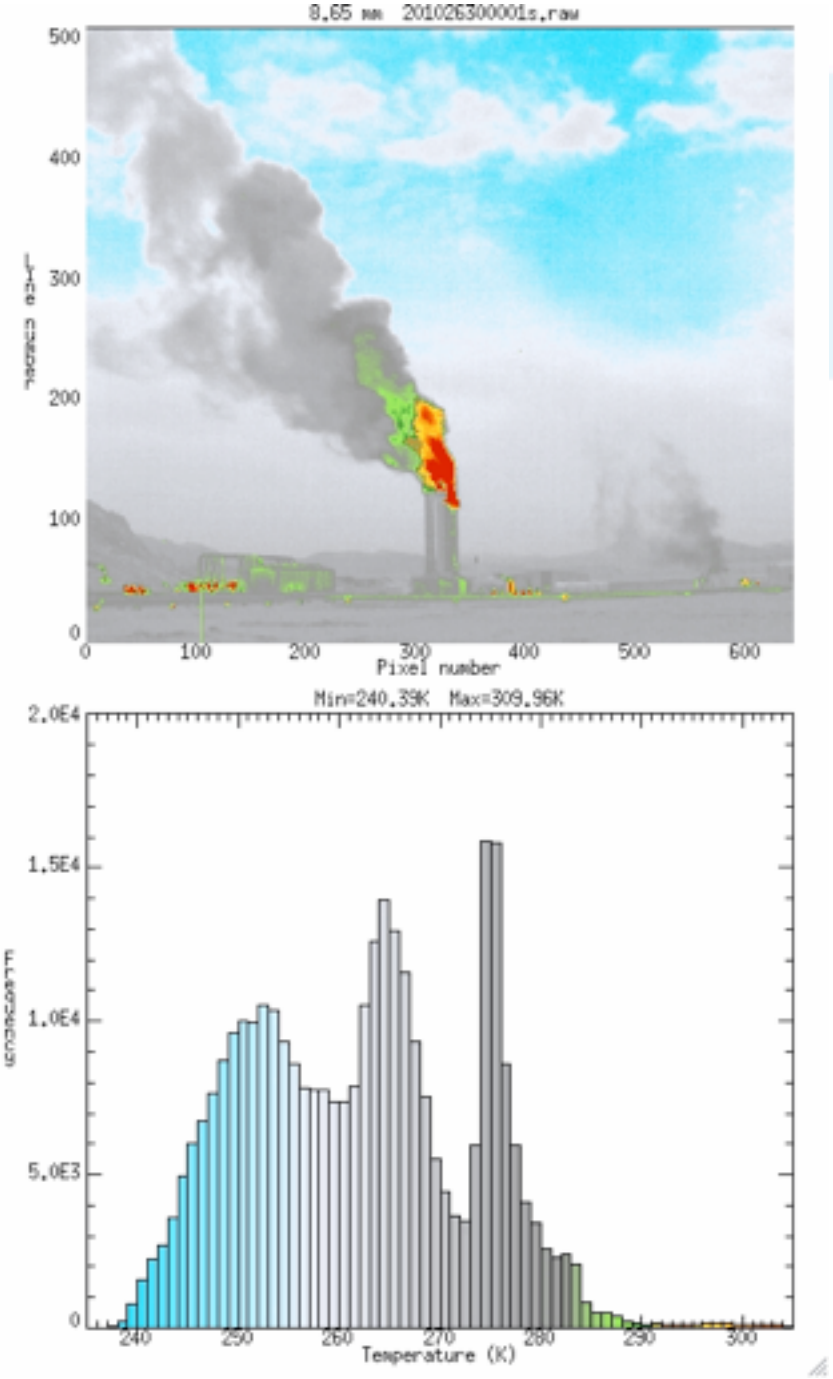
8.65 mm 201026300001s.raw
Pixel number
Min=240.39K Max=309.96K
Temperature (K)

Arenal






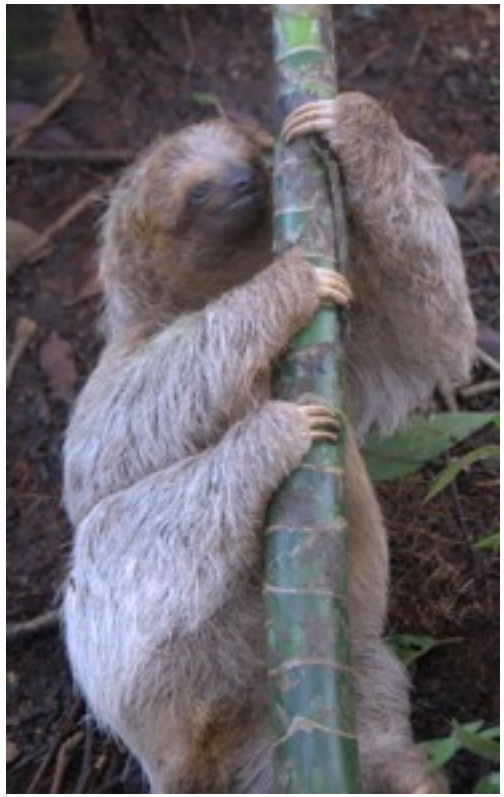

NILU

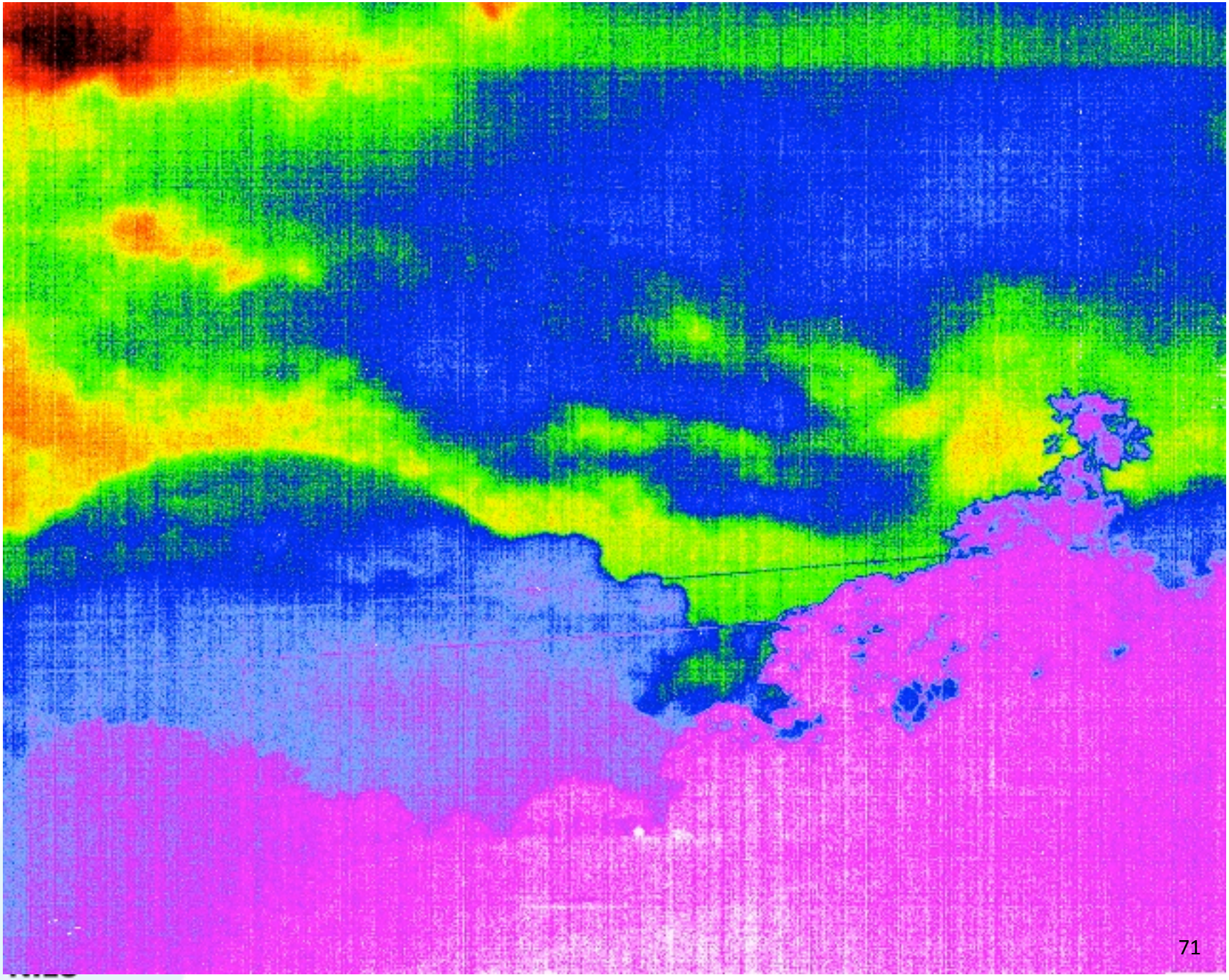

Turrialba

Andres Diaz, Simon Carn, Helen Thomas, Taryn Lopez, Vladimir Conde, Kelby Hicks, Fred Prata

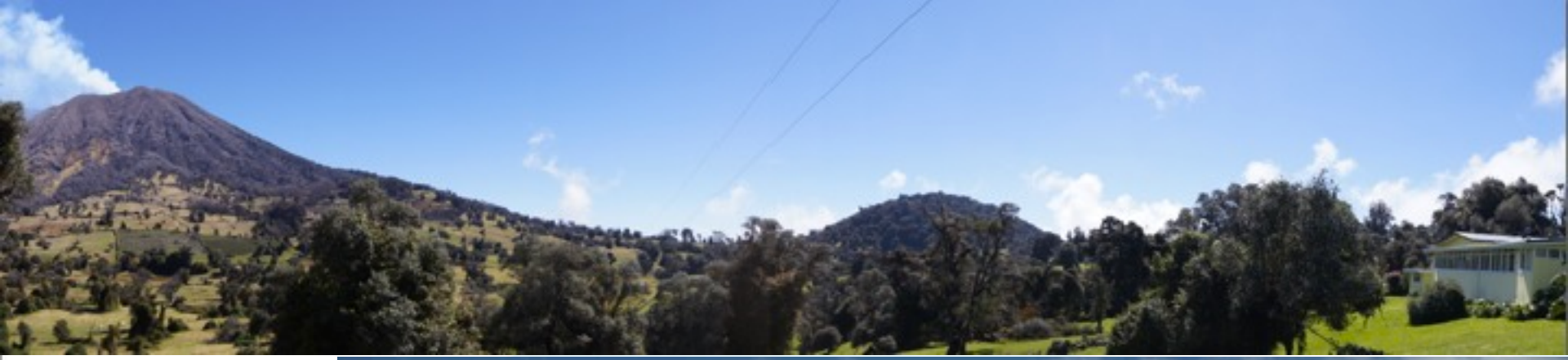

A1
CARTA

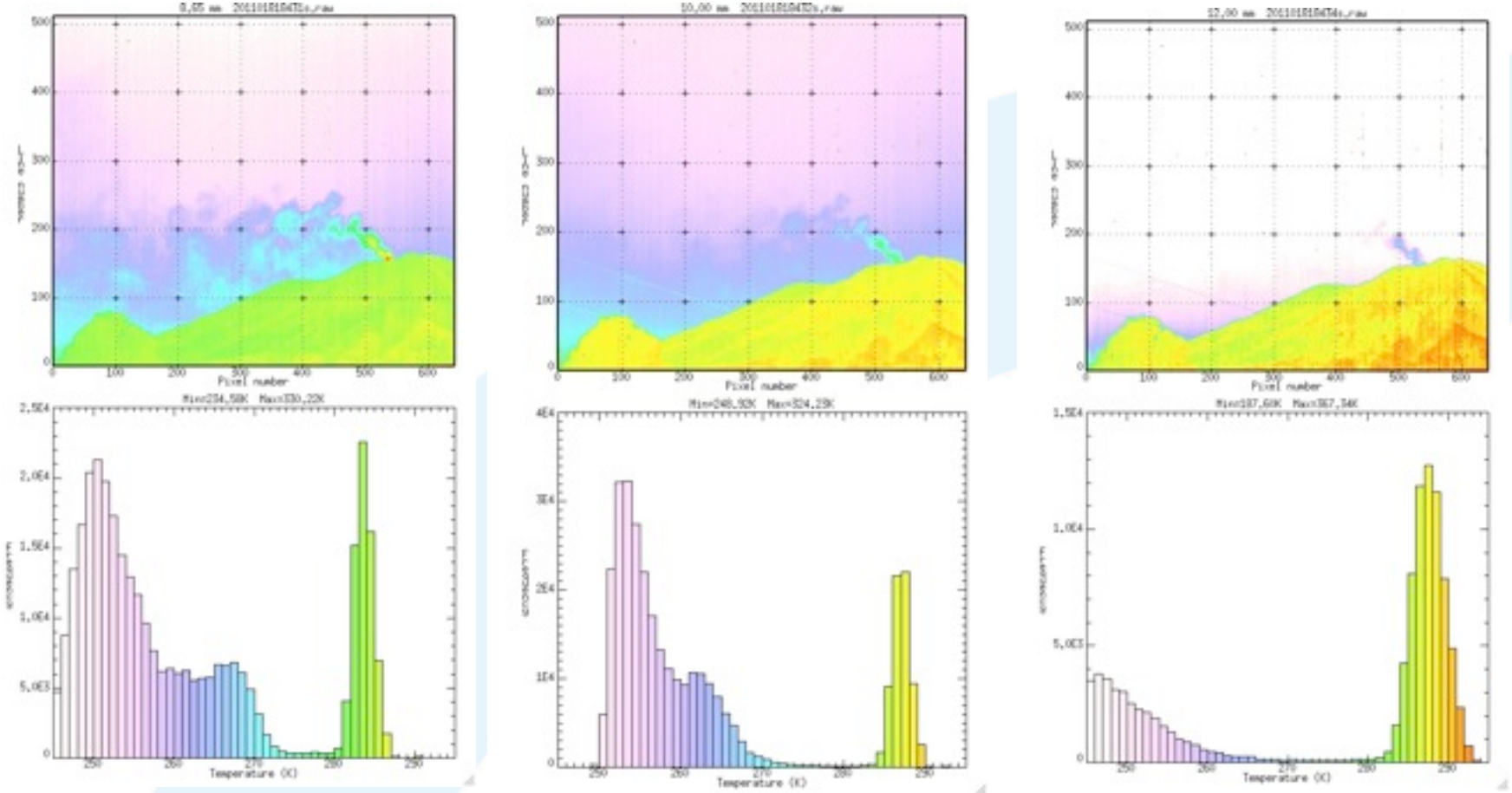
Pixel number
Temperature (K)

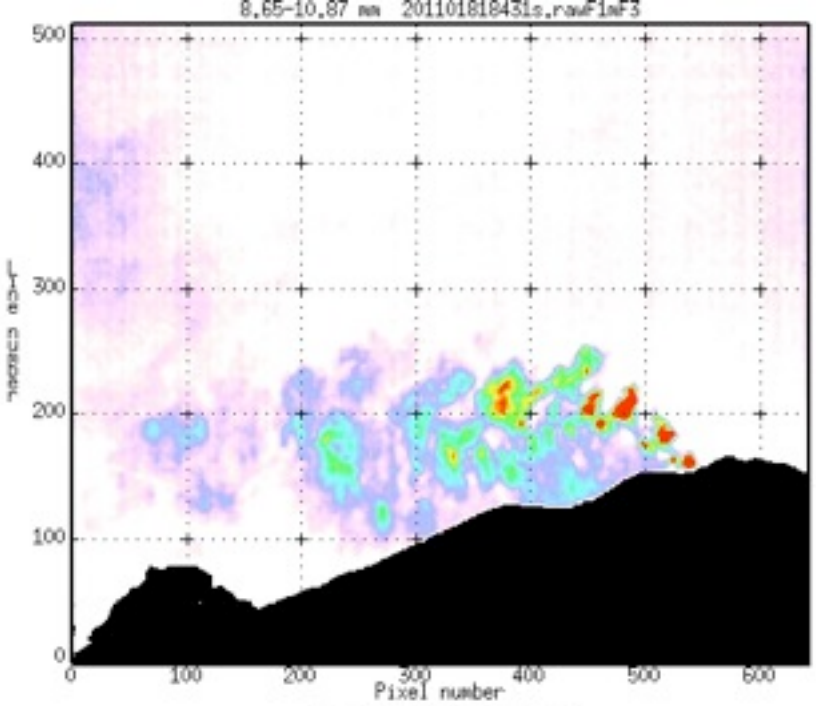
8.65-10.87 mm 20110181843is.rawFlaF3
Pixel number

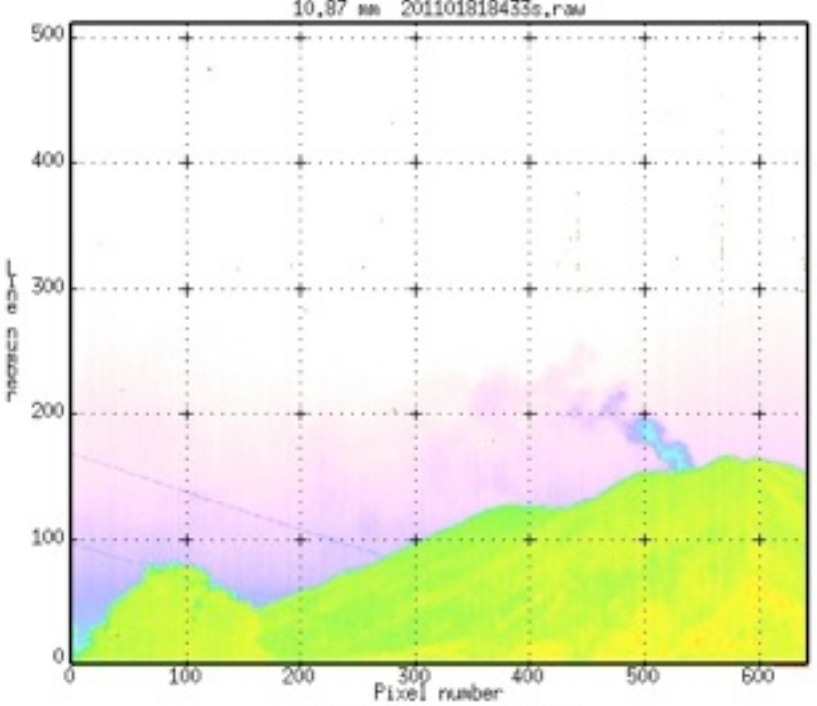
10.87 mm 20110181843is.raw
Pixel number

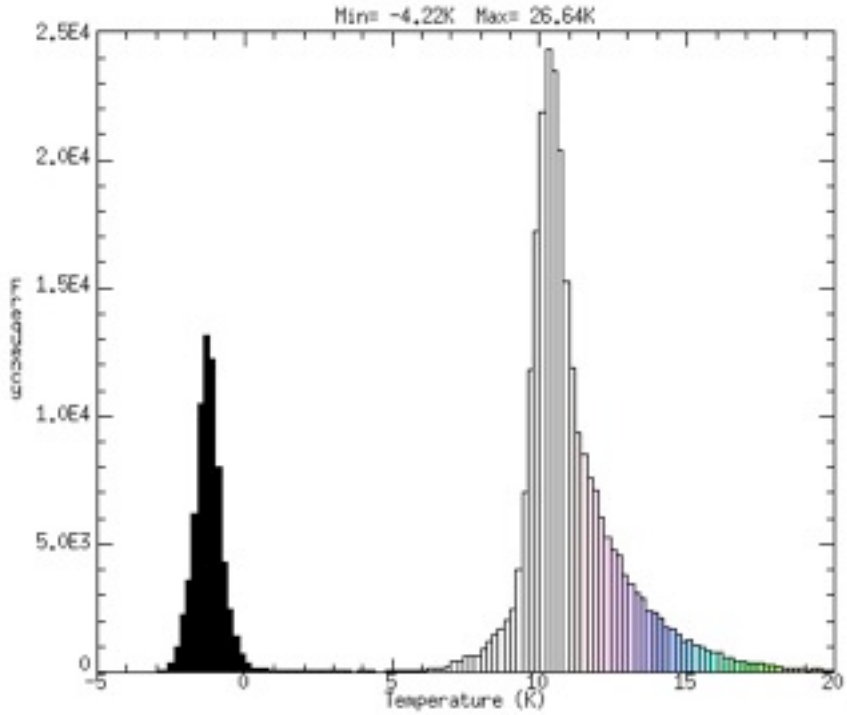
Min= -4.22K Max= 26.64K
Temperature (K)

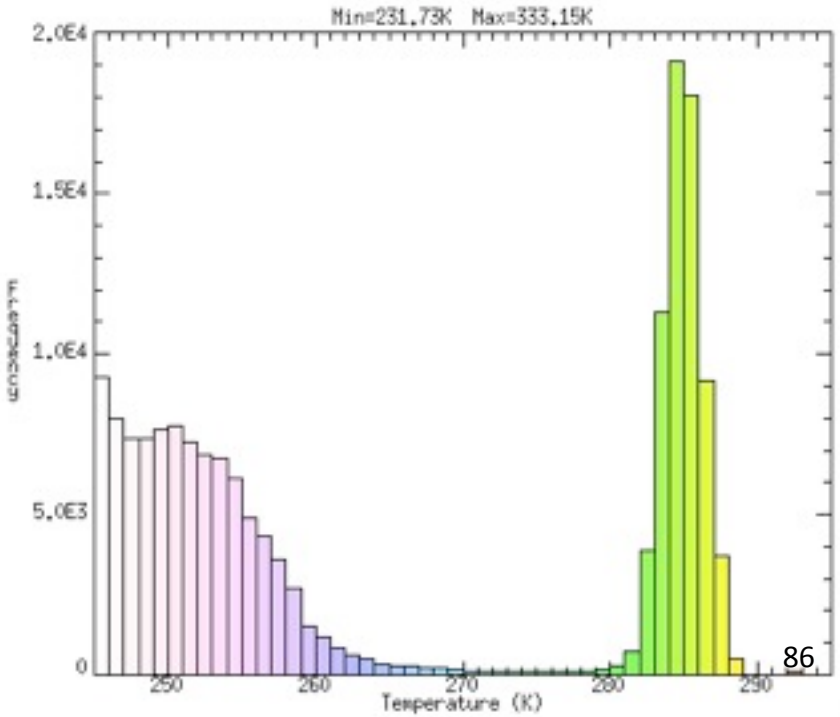
Min=231.73K Max=333.15K
Temperature (K)

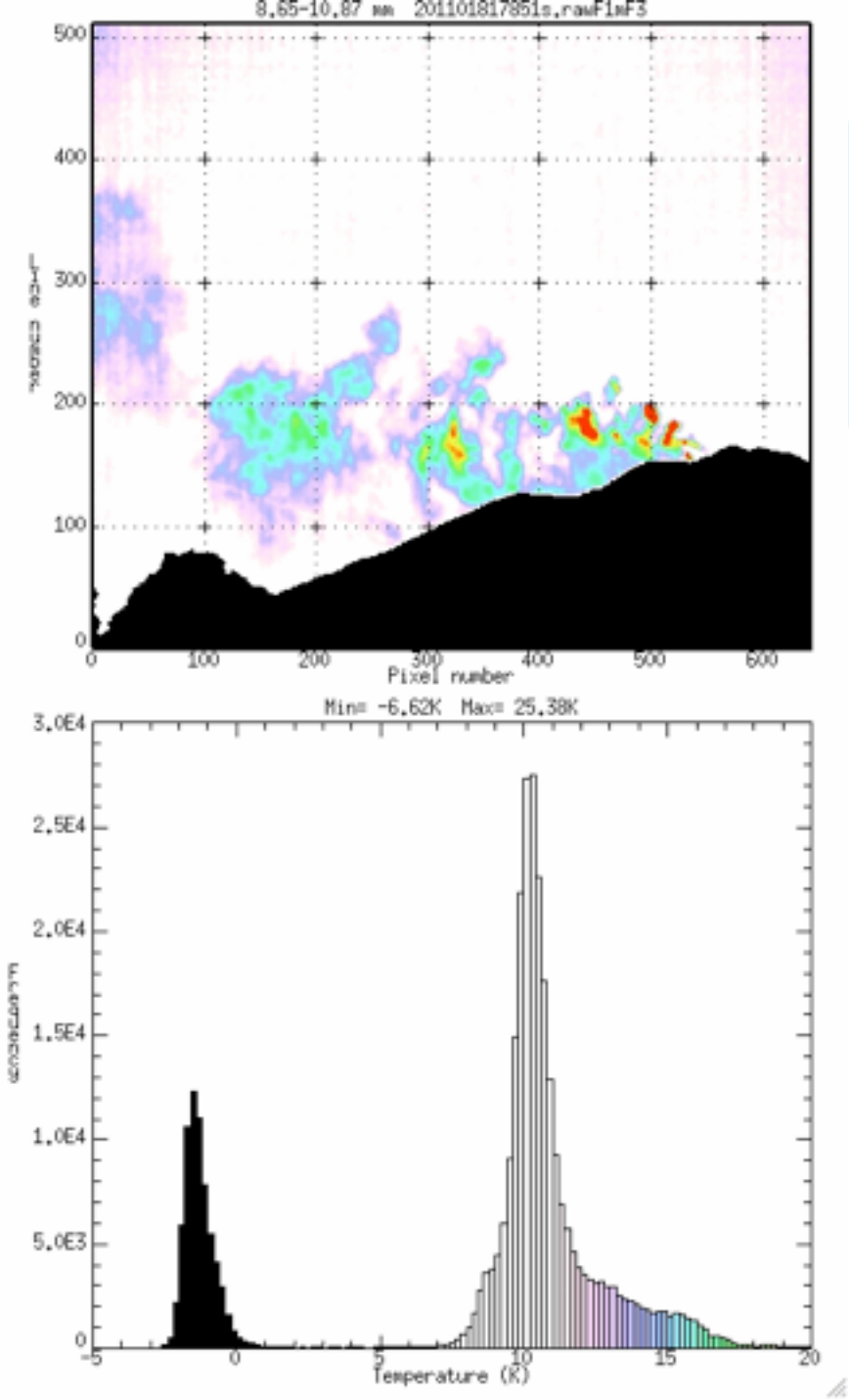
8.65-10.87 mm 201101817851s.rawF1wF3
500
400
300
200
100
0
0
100
200
300
400
500
600
Pixel number
Min= -6.62K Max= 25.38K
3.0E4
2.5E4
2.0E4
1.5E4
1.0E4
5.0E3
0
-5
0
5
10
15
20
Temperature (K)

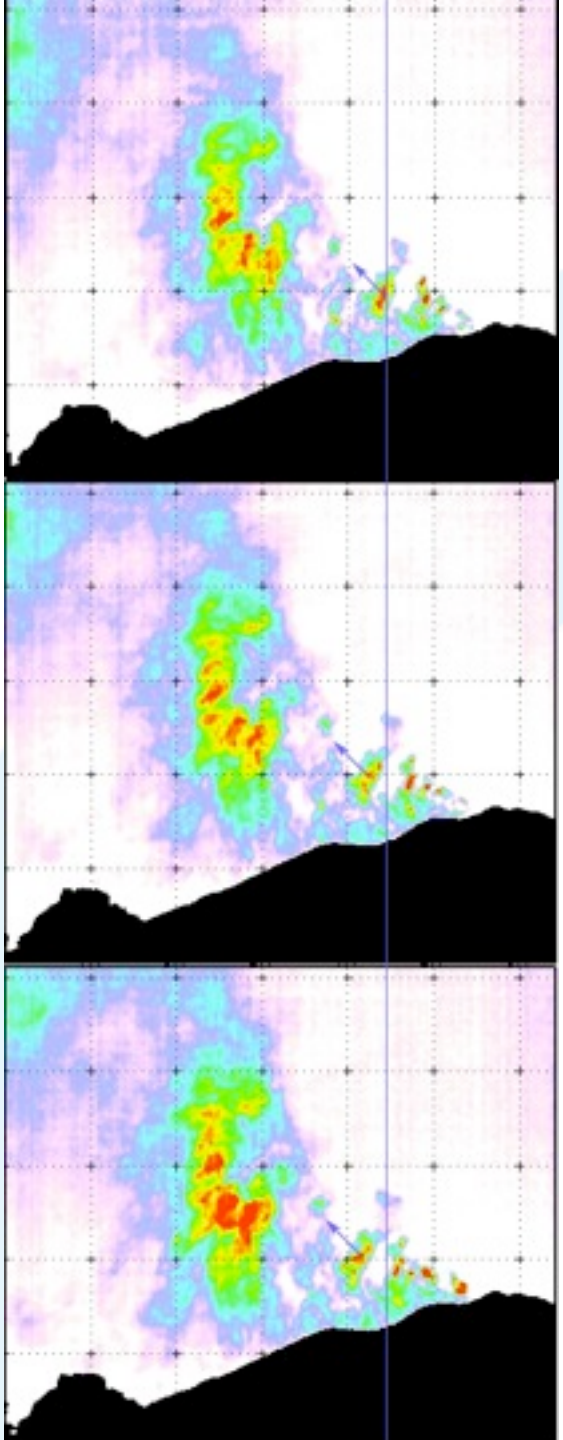

Tracking movement of individual features allows plume speed and direction (plume velocity) to be determined. Thus, fluxes can be inferred.

Poas


NILU

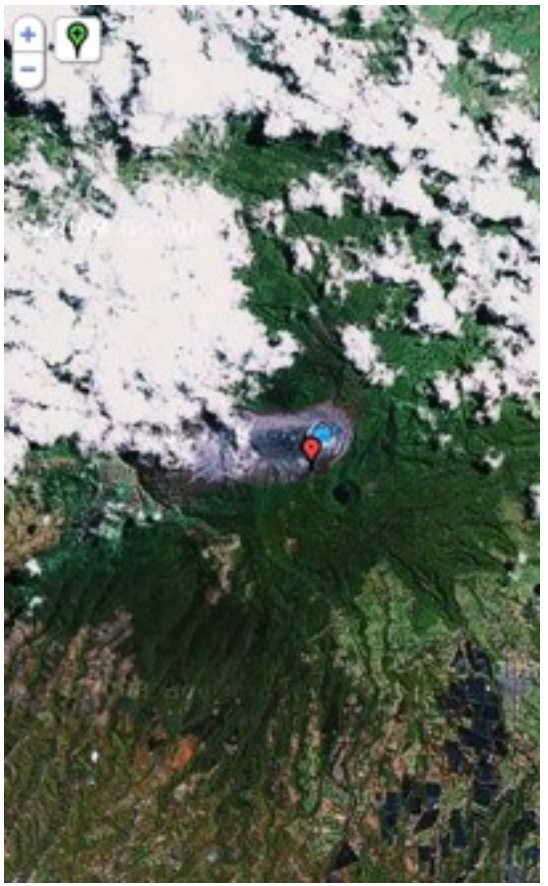


NILU

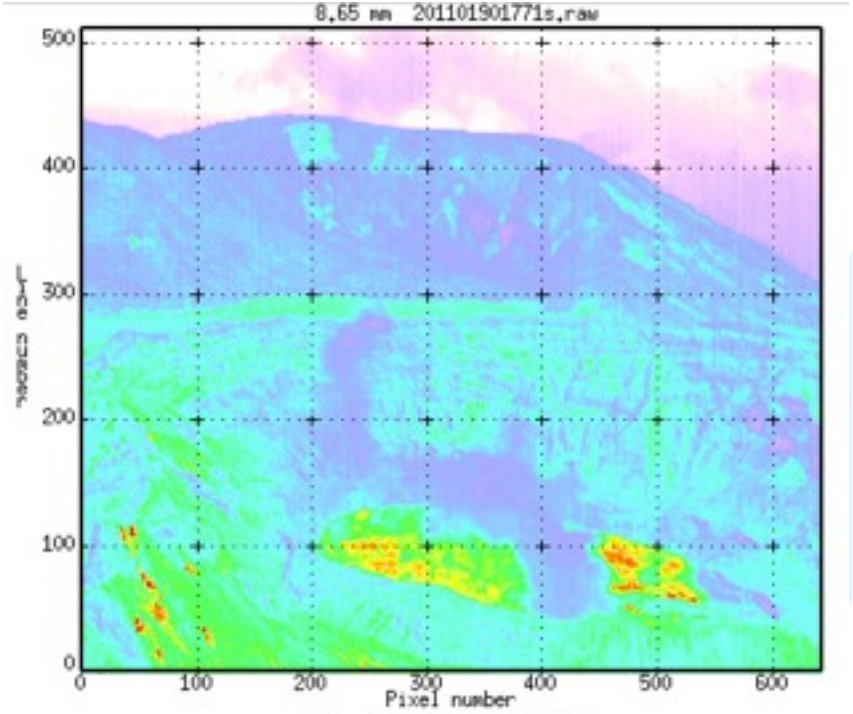
8.65 mm 201101901771s.raw
Pixel number

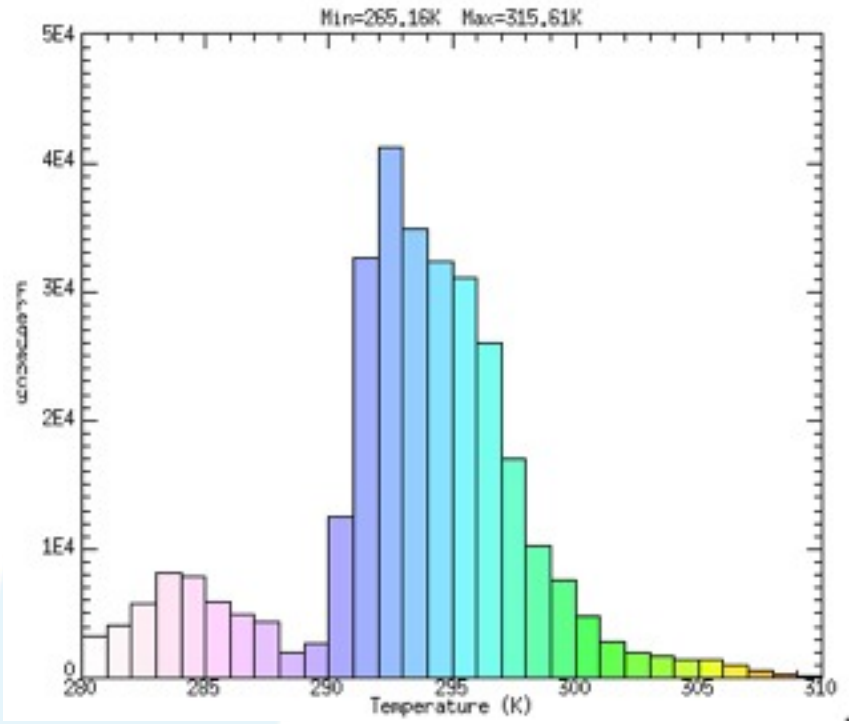
Min=265.16K Max=315.61K
Temperature (K)

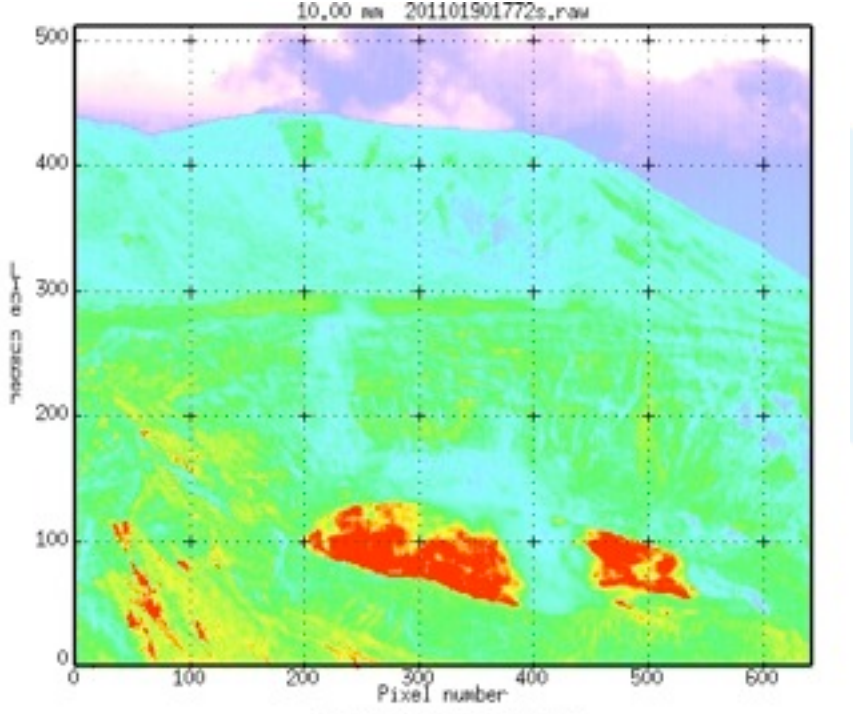
10.00 mm 201101901772s.raw
Pixel number

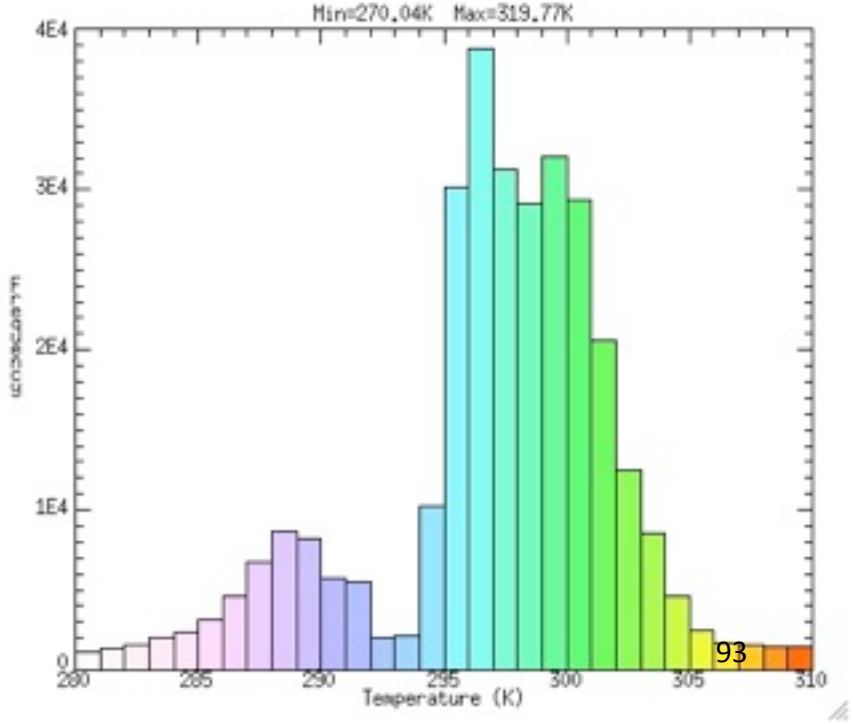
Min=270.04K Max=319.77K
Temperature (K)

Application to the atmosphere

TGRS-00408-2004 Accepted for publication in the *IEEE Transactions on Geoscience and Remote Sensing*, June 2

Cloud Statistics Measured With the Infrared Cloud Imager (ICI)

Brentha Thurairajah, *Member, IEEE* and Joseph A. Shaw, *Senior Member, IEEE*

Abstract— **The Infrared Cloud Imager (ICI) is a ground-based thermal infrared imaging system that measures spatial cloud statistics with a 320×240-pixel uncooled microbolometer detector array. Clouds are identified from the residual radiance that remains after water vapor emission is removed from radiometrically calibrated sky images (the water vapor correction relies on measurements of precipitable water vapor and near-surface air temperature). Cloud amount, the percentage of an ICI image containing clouds, is presented for data from Atmospheric Radiation Measurement (ARM) sites at Barrow, Alaska in February–April 2002, Lamont, Oklahoma in February–April 2003, and Barrow, Alaska in March–April 2004.**

Spatial cloud distribution also is a key factor in u
and modeling cloud radiation feedback mechanism

While satellite sensors achieve global covera
based sensors provide improved radiometric cont
clouds and the background. This is especially
latitudes, where satellites have difficulty di
between clouds and the underlying surface [3]. O
based cloud measuring instruments generally are
angle, spatially resolving passive imagers or ze
active sensors. For example, the Total Sky Imag
measures visible skylight (~450-650 nm) from th

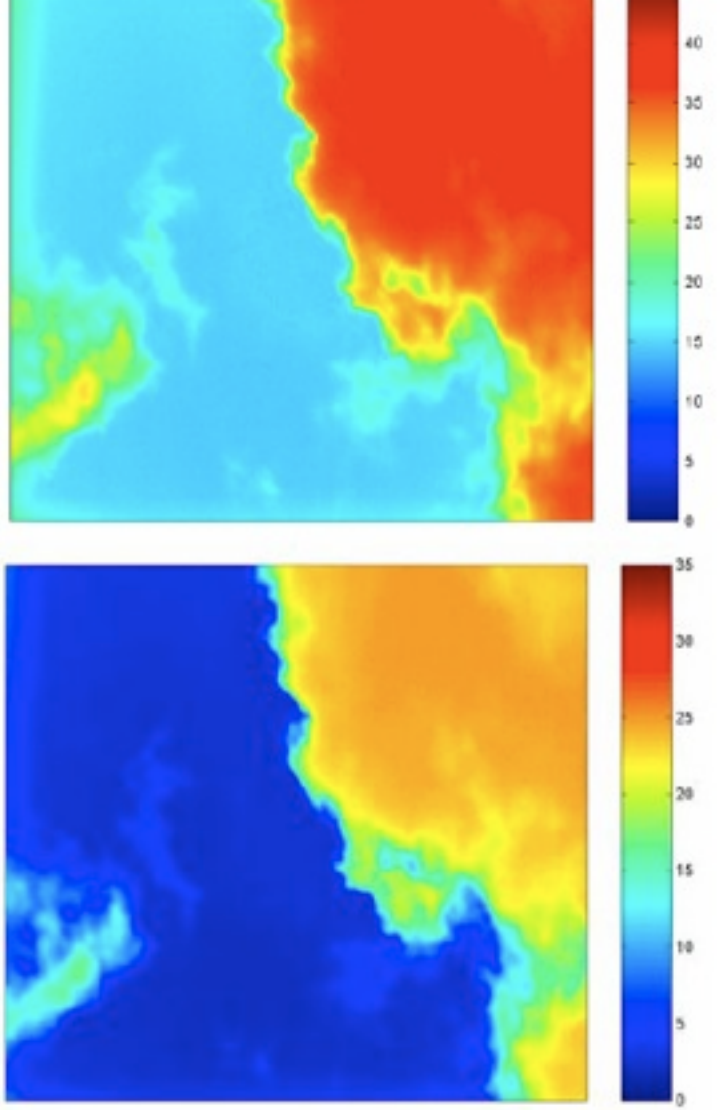

Figure 5. ICI images before (top) and after (bottom) the temperature-dependent water vapor correction (note the different scales). The images are from Oklahoma on April 20, 2003, with air temperature = 17°C and PWV = 1.3 cm. The clear-sky region in the bottom image has residual radiance less than 2 W/(m^2 sr), below the default cloud threshold of 2.65 W/(m^2 sr), indicating successful removal of non-cloud atmospheric emission.

NILU

FIRST - Advanced Imaging Spectroradiometer

- Imaging Spectroradiometer
- Commercial Off-the-Shelf

Fourier Transform Technology
- LWIR: 8-12 μm
- MWIR: 3-5μm
- MWIR-E: 1.5-5.5μm

- Cooled FPA 320 × 256
- IFOV of 0.35 mrad
- Adjustable spectral resolution:
  - 0.24 – 150 cm^{-1}
- Real-time FFT
- Internal calibration blackbodies
- Boresight video

NILU